Supplemental Material

Genome-wide cooperation by HAT Gcn5, remodeler SWI/SNF, and chaperone Ydj1 in promoter nucleosome eviction and transcriptional activation

Hongfang Qiu[1,†], Răzvan V. Chereji[2,†], Cuihua Hu[1], Hope A. Cole[2], Yashpal Rawal[1], David J. Clark[2,*], and Alan G. Hinnebusch[1,*]

[1]Laboratory of Gene Regulation and Development, *Eunice Kennedy Shriver* National Institute for Child Health and Human Development, National Institutes of Health, Bethesda, Maryland 20892, USA
[2]Program in Genomics of Differentiation, *Eunice Kennedy Shriver* National Institute for Child Health and Human Development, National Institutes of Health, Bethesda, Maryland 20892, USA
[†]These authors contributed equally to this work.
[*]To whom correspondence should be addressed. E-mail addresses: ahinnebusch@nih.gov (A.G.H.), clarkda@mail.nih.gov (D.J.C.)

Contents

Supplemental Methods

Yeast strain constructions

WT strain BY4741 and *kanMX*-marked deletion derivatives were described previously (Winzeler et al. 1999) and purchased from Research Genetics, and all deletions in these strains were verified by PCR analysis of genomic DNA either previously (Swanson et al. 2003) or in the current study. Double mutants harboring *hphMX4*-marked deletions were produced from the appropriate single mutants containing a *kanMX4*-marked deletion by gene replacement of the relevant WT chromosomal gene with a cassette containing *hphMX4* in place of the CDS, amplified from plasmid pAG32 with the appropriate primers (Goldstein and McCusker 1999). The single mutants used in these gene replacements were complemented by a *URA3* plasmid containing the WT allele of the *kanMX*-deleted gene, which was evicted by growth on 5-FOA after generating the second *hphMX*-marked second deletion. We verified that the slow-growth phenotypes of the *ydj1*Δ*snf2*Δ and *ydj1*Δ*gcn5*Δ double mutants could be partially complemented by *YDJ1* on plasmid pHQ2063 (construction of this plasmid described below). To construct HQY1602 and HQY1603, *hsc82*Δ*::kanMX4* strain 771 was transformed with plasmid pHQ2062 (*HSP82, URA3*) and chromosomal *HSP82* was replaced with *hsp82*Δ*::hphMX4* to produce HQY1601; which was subsequently transformed with pHQ2066 (*hsp82-T101I, LEU2*) or pHQ2067 (*hsp82-G170D, LEU2*), and derivatives lacking pHQ2062 were selected on 5-FOA medium. Strains carrying P_{TET}-*SNF2* were constructed by gene replacement with *HIS3::*P_{TET}-*SNF2* DNA fragments PCR-amplified from plasmid pHQ2078 using forward primer: 5'-*TGGACCTTTTGTATATAAATCATCGGGAAGGTCAGCTATTCTGTTGTTTCTCT-AATCGCGACTTTCTGCT*CAGCTGAAGCTTCGTACGC 3' (with *SNF2* promoter sequences -100 to -31 italicized) and reverse primer: 5'- *TCAAATGCTGCCATCTTAAATAGCAGCGGTTG-ACCTCTTCGTTGCTAAATTGACGCTGTGGTATGTTCAT*ATAGGCCACTAGTGGATCTG 3' (with *SNF2* CDS sequences +70 to +1 italicized). Replacement of *SNF2* promoter with the *HI3MX-tTA-tetO*$_2$ cassette was confirmed by PCR analysis and the Western blot analysis of Snf2 in Fig. S5.

Plasmids

A ∼2.25 kb fragment of *YDJ1* containing the 635 (5') or 381bp (3') of flanking sequences was PCR-amplified from WT genomic DNA with Asp718 and XbaI restriction sites added at the 5' and 3' ends, and cloned into YCplac33 to produce pHQ2063. A ∼3.2 kb fragment of *HSP82* containing the 2130bp CDS and 800 (5') or 237 bp (3') of flanking sequences was PCR-amplified from WT genomic DNA with BamHI and SalI restriction sites added at the 5' and 3' ends, and cloned into YCplac33 to produce pHQ2062. For construction of *hsp82-T101I*, a ∼1.1 kb fragment containing the 5' portion of *HSP82* containing a mutation encoding the T101I substitution (introduced using the mutagenic oligonucleotide reverse primer) and BamHI and Eco47III restriction sites at the 5' and 3' ends, and a ∼2.1 kb fragment of the 3' portion of *HSP82* with Eco47III and SalI restriction sites at the 5' and 3' ends, were PCR-amplified from WT genomic DNA. These two PCR fragments were digested with BamHI and Eco47III, or Eco47III and SalI, respectively, and inserted into YCplac111 between the BamHI and SalI sites to produce pHQ2066. Similarly, for construction of *hsp82-G170D*, a ∼1.3 kb fragment containing the 5' portion of *HSP82* encoding the *G170D* mutation and BamHI and FspI restriction sites at the 5' and 3' ends, and a ∼1.9 kb fragment of the 3' portion of *HSP82* with Eco47III and SalI restriction sites at the 5' and 3' ends, were PCR-amplified from WT genomic DNA. The PCR fragments were digested with BamHI and FspI or Eco47III and SalI, respectively, and inserted into YCplac111 between the BamHI and SalI sites to produce pHQ2067. A BglII-EcoRI

kanMX fragment of the *kanMX-tTA-tetO$_2$* cassette of pCM224 (Bellí et al. 1998) was replaced with the *HIS3MX6* BglII-EcoRI fragment from pFA6a-3HA-His3MX6 (Longtine et al. 1998) to produce pHQ2078.

Paired-end sequencing of chromatin immunoprecipitates (PESCI)

The procedure described by (Cole et al. 2014) for preparing DNA libraries for Illumina pair-end sequencing was followed with the following modifications. Immediately prior to harvesting, cells were fixed with 1% formaldehyde (20 min at room temperature) and glycine was added to 0.3 M for 5 min. Cells were collected by centrifugation, washed twice with ice-cold Tris-buffered saline (pH 7.5), and cell pellets were stored at -80°C. Each frozen cell pellet from 100 mL culture was suspended in 0.4 mL FA buffer (50 mM Hepes-KOH [pH 7.5], 140 mM NaCl, 1 mM EDTA, 1% Triton X-100, 0.1% sodium deoxycholate, 1 mM PMSF, 1 μg/mL leupeptin, 1 μg/mL pepstatin A and 10 μg/mL aprotinin), 0.6 mL glass beads were added, and cells were vortexed for 45 min at 4°C. The beads were removed, FA buffer added to 1 mL, and the cell lysate was spun at 14,000 rpm for 10 min at 4°C. The pellet was resuspended in 1 mL FA buffer and spun again. The final pellet was resuspended in 0.5 ml FA buffer and sonicated using a Diagenode Bioruptor 300 at 4°C with 40 cycles of 30 s at high power and 30 s at rest, with a 15 min cooling period after 20 cycles. Debris was removed by spinning for 20 min at 14,000 rpm at 4°C. The supernatant was divided into 100μL aliquots and stored at -80°C. A 100 μL aliquot of supernatant was adjusted to 200 μL by adding 100 μL FA buffer, 4 μL of 1M Tris (pH8.0), 2 μL of 0.5 M EDTA and 10 μL of 10% SDS and incubated at 65°C overnight to reverse the cross-links. DNA was purified by treating with proteinase K (add 100μg proteinase K) for 4 h at 55°C, extracting twice with an equal volume of chloroform, and precipitating with 0.7 volume of isopropanol and washed with 1 mL of 70% ethanol. Purified DNA was quantified using the NanoDrop ND-1000. For immunoprecipitation, anti-H3 antibody (1μg, Abcam ab1791) or anti-Rpb3 antibody (1.5 μL, NeoClone, W0012) was first incubated in 200 μL FA buffer for 3 h with 50 μL of Dynabeads anti-Rabbit IgG (Invitrogen, Cat# 11204D) or 50 μL of Dynabeads Pan Mouse IgG (Invitrogen, Cat# 110.42), respectively, that had been pre-washed twice with 500 μL PBS/BSA buffer. The resulting anti-H3 or anti-Rpb3 conjugated Dynabeads were washed twice with 500 μL PBS/BSA, and mixed with chromatin extract containing 2.5 μg DNA and FA buffer at a final volume of 200 μL, and rotated at 4°C for 3 h. The beads were washed twice with 1 mL FA buffer containing 0.025% SDS, once with 1 mL FA buffer, twice with 1 mL Wash buffer II (50 mM Hepes-KOH [pH7.5], 500 mM NaCl, 1 mM EDTA, 1% Triton X-100 and 0.1% sodium deoxycholate), twice with 1 mL Wash buffer III (10 mM Tris-HCl [pH8.0], 250 mM LiCl, 1 mM EDTA, 0.5% NP-40 and 0.5% sodium deoxycholate), and once with 1 mL TE. Bound chromatin was eluted with 100 μL elution buffer (50 mM Tris-HCl [pH8.0], 10 mM EDTA and 1% SDS) at 65°C for 15 min and the eluate collected. Elution was repeated with 150 μL elution wash buffer (10 mM Tris-HCl [pH8.0], 1 mM EDTA and 0.67% SDS) for 10 min at 65°C. The eluates were pooled and incubated at 65°C overnight to reverse the cross-links, followed by proteinase K digestion (0.4 mg/mL, 4 h, 55°C). The digest was cooled, mixed with one-fifth volume of 5M potassium acetate, and extracted twice with an equal volume of chloroform. DNA was precipitated with 0.7 volume isopropanol in the presence of 15 μg glycoBlue (Ambion/Invitrogen), washed once with 70% ethanol and dissolved in 45 μL TE (10 mM Tris-HCl [pH 8.0], 0.1 mM sodium EDTA). Immunoprecipitated purified DNA was repaired as described (Cole et al. 2012), purified using a Qiagen PCR column and eluted with 50 μL TE. A 5'-phosphate and a 3'-dA were added, followed by ligation to Illumina paired-end adaptor (cat. #1005711) (Cole et al. 2012). The adaptor-ligated immunoprecipitated

DNA (5 μL for anti-H3 or 7.5 μL for anti-Rpb3) was subjected to PCR (22 cycles for H3 and 25 cycles for Rpb3) in 50 μL with Illumina paired-end primers (InPE1.0 and InPE2.0) and an index primer at the concentrations recommended by the vendor. DNA was purified using a Qiagen PCR column. To remove primer-dimers and larger DNA fragments, 200-450 bp fragments were resolved by gel electrophoresis using a precast 2% agarose gel and E-Gel system (Invitrogen) and purified using Zymoclean Gel DNA Recovery Kit, and the final concentration was determined with a Qubit 2.0 Fluorometer (Invitrogen). DNA fragment size was verified by agarose gel electrophoresis prior to sequencing.

Supplemental Results

Comparison of conventional H3 ChIP and H3 ChIP-seq results for *ARG1*, *HIS4*, *ARG4* and *CPA2*

Overall, there is good agreement between the measurements of H3 occupancy by ChIP-seq (Figs. S13-S15, summarized in Fig. S18) and conventional ChIP (Fig. S3B) for the 4 canonical target genes *ARG1*, *HIS4*, *ARG4* and *CPA2*. Both approaches implicated only Ydj1 and Snf2 at *ARG1* and all three co-factors at *HIS4*. Whereas conventional ChIP revealed roles for all three co-factors at *ARG4* (Figs. 1E & S3B), only Gcn5 and Ydj1 were implicated at this gene by ChIP-seq measurements (Fig. S18). However, *snf2*Δ produced a defect in H3 eviction at *ARG4* in ChIP-seq assays (Fig. S13A) with a p-value of 0.09 (Fig. S18, row 9), just above the threshold of $p<0.05$ used to construct the Venn diagram in Fig. 4C. Given the high precision of conventional ChIP measurements for *ARG4* (Fig. S4A), we elected to place *ARG4* among the group of genes employing all three co-factors for H3 eviction (Fig. 4C). Whereas conventional ChIP and ChIP-seq measurements both implicated Gcn5 and Snf2 at *CPA2*, the role of Ydj1 was clearly established only by conventional ChIP analysis. ChIP-seq measurements for *CPA2* in Fig. S13D are suggestive of an additive effect of *snf2*Δ and *ydj1*Δ, consistent with Ydj1 functioning at *CPA2*; however, because this was not observed for the corresponding *gcn5*Δ/*ydj1*Δ ChIP-seq data in Fig. S14D, we refrained from implicating Ydj1 at *CPA2* in Fig. 4C.

Supplemental Figures

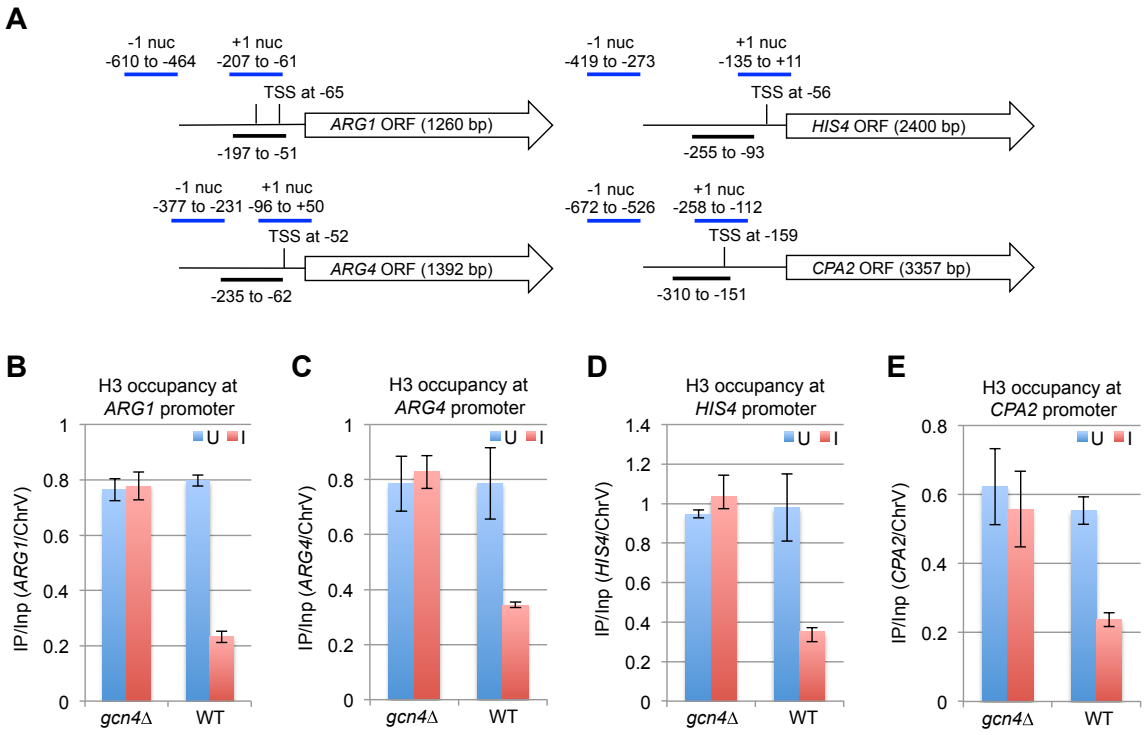

Supplemental Figure S1. SM-induced depletion of histone H3 from promoters of four canonical Gcn4 target genes requires Gcn4. (A) Sequence coordinates of primers for conventional ChIP analysis of promoter occupancies relative to the ATG start codon. Coordinates of TSS were obtained from (Xu et al. 2009), and coordinates of -1 and +1 nucleosomes determined as described in Fig. S10B. (B-E) Promoter occupancies of H3 measured by conventional ChIP in the indicated strains cultured in SC medium (U) or treated with sulfometuron methyl (SM) for 30 min to induce Gcn4 (I). Cross-linked chromatin was immunoprecipitated with anti-H3 antibodies and DNA from immunoprecipitated (IP) and input samples was subjected to PCR in the presence of [33P]-dATP to amplify radiolabeled fragments of the relevant gene or non-transcribed sequences from chromosome V analyzed as a control, which were resolved by PAGE and quantified by phosphorimaging analysis. Ratios of target gene to ChrV signals in IP samples were normalized to the corresponding ratios for Input samples to yield occupancy values. Mean (+/-SD) values were calculated from 3 biological replicates.

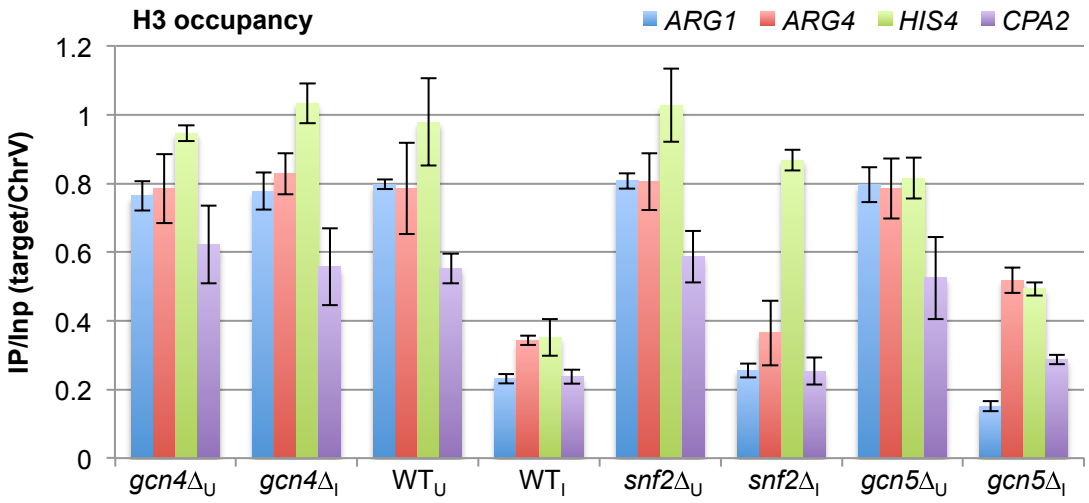

Supplemental Figure S2. Snf2 and Gcn5 promote H3 eviction from promoters of Gcn4 target genes only under inducing conditions. Conventional ChIP analysis of H3 in the indicated strains under inducing (I) or uninducing (U) conditions, conducted as in Fig. 1. Mean (±SD) values were calculated from 3 biological replicates.

A

		H3 EDI				Gcn4 occupancy (%WT)			
	Mutant	*ARG1*	*ARG4*	*HIS4*	*CPA2*	*ARG1*	*ARG4*	*HIS4*	*CPA2*
1	*gcn4Δ*	1	1	1	1	N/A	N/A	N/A	N/A
2	*gal11Δ/med15Δ*	-0.1	-0.02	-0.12	-0.11	1.2	1.2	1.0	1.1
3	*snf2Δ*	-0.16	0.15	0.83	-0.05	2.1	1.6	1.0	1.5
4	*sth1-3*	-0.08	0.05	-0.1	-0.04				
5	*ada1Δ*	-0.09	0.61	0.25	0.1	1.8	1.1	1.0	0.98
6	*gcn5Δ*	-0.31	0.39	0.11	0.05	2.2	1.4	1.4	1.3
7	*asf1Δ*	-0.27	-0.09	-0.15	-0.2	1.7	1.4	2.1	1.8
8	*rrt109Δ*	-0.11	-0.08	0.08	-0.18				
9	*spt16-169*	0.29	0.37	N/A	0	0.41	0.31	N/A	0.31
10	*nap1Δ*	-0.12	-0.14	-0.21	-0.25				
11	*yta7Δ*	0	0.14	0.32	-0.02	1.4	1.2	1.1	1.2
12	*hsc82Δ*	-0.09	-0.1	-0.12	-0.2				
13	*hsc82Δ hsp82-T101I*	-0.15	-0.02	-0.02	-0.03				
14	*hsc82Δ hsp82-G170D*	-0.1	-0.06	-0.16	-0.03				
15	*ssa1Δ ssa2Δ*	0.19	0.13	0.14	0.13	0.84	0.86	0.68	0.91
16	*ydj1Δ*	0.31	0.13	-0.01	-0.07	0.98	1.0	1.1	1.2
17	*htz1Δ*	0.14	0.13	0.11	0				

< 0	0-0.14	0.15-0.39	0.40-0.54	0.55-0.69	0.70-0.84	>0.84

B

		H3 EDI				Gcn4 occupancy (%WT)			
	Mutant	*ARG1*	*ARG4*	*HIS4*	*CPA2*	*ARG1*	*ARG4*	*HIS4*	*CPA2*
1	*gcn4Δ* (-dox)	1	1	1	1				
2	*snf2Δ*	-0.16	0.15	0.83	-0.05	2.1	1.6	1.0	1.5
3	*gcn5Δ*	-0.31	0.39	0.11	0.05	2.2	1.4	1.4	1.3
4	*ydj1Δ*	0.31	0.13	-0.01	-0.07	0.98	1.0	1.1	1.2
5	*gcn5Δ ydj1Δ*	0.06	0.68	0.41	0.29	2.0	1.1	1.4	1.5
6	*snf2Δ ydj1Δ/lcGCN4*	0.38	0.41	0.73	0.37	0.97	1.1	0.98	1.2
7	*P_{TET}-SNF2* (+Dox)	-0.04	0.17	0.83	0.05	1.3	1.2	1.4	1.3
8	*P_{TET}-SNF2 gcn5Δ* (+Dox)	-0.14	0.7	1.05	0.23	1.6	0.99	0.82	1.4
9	*P_{TET}-SNF2 gcn5Δ ydj1Δ/lcGCN4* (+Dox)	0.35	0.82	0.92	0.51	1.3	0.94	0.9	1.4

Supplemental Figure S3. Summary of H3 EDI values and Gcn4 occupancies at canonical Gcn4 target genes in different mutants. (A-B) H3 and Gcn4 occupancies were determined by conventional ChIP analysis, as in Fig. 1A-D, and EDI values were calculated as $(H3_{I(mut)} - H3_{I(WT)})/(H3_{I(gcn4\Delta)} - H3_{I(WT)})$, where $H3_{I(mut)}$, $H3_{I(WT)}$, and $H3_{I(gcn4\Delta)}$ signify H3 occupancies in induced mutant, induced WT cells, or induced *gcn4Δ* cells, respectively. Mean EDI values were determined from the EDIs calculated from 3 or more biological replicates, as shown for selected mutants in Fig. S4A, with all SEMs <20% of the mean values with 3 exceptions: *gcn5Δ* at *HIS4* (SEM/mean=0.68), *gcn5Δ* at *CPA2* (SEM/mean=0.55), and *gcn5Δydj1Δ* at *ARG1* (SEM/mean=0.24). EDI ranges are color-coded as indicated. Mean Gcn4 occupancies normalized to those measured in WT cells were determined from replicate experiments as described in Figs. 1C & E, with all SEMs <20% of the mean values shown. N/A, not applicable. H3 and Gcn4 ChIP analyses were not conducted for the *spt16-169* mutant because it harbors a mutant *HIS4* promoter.

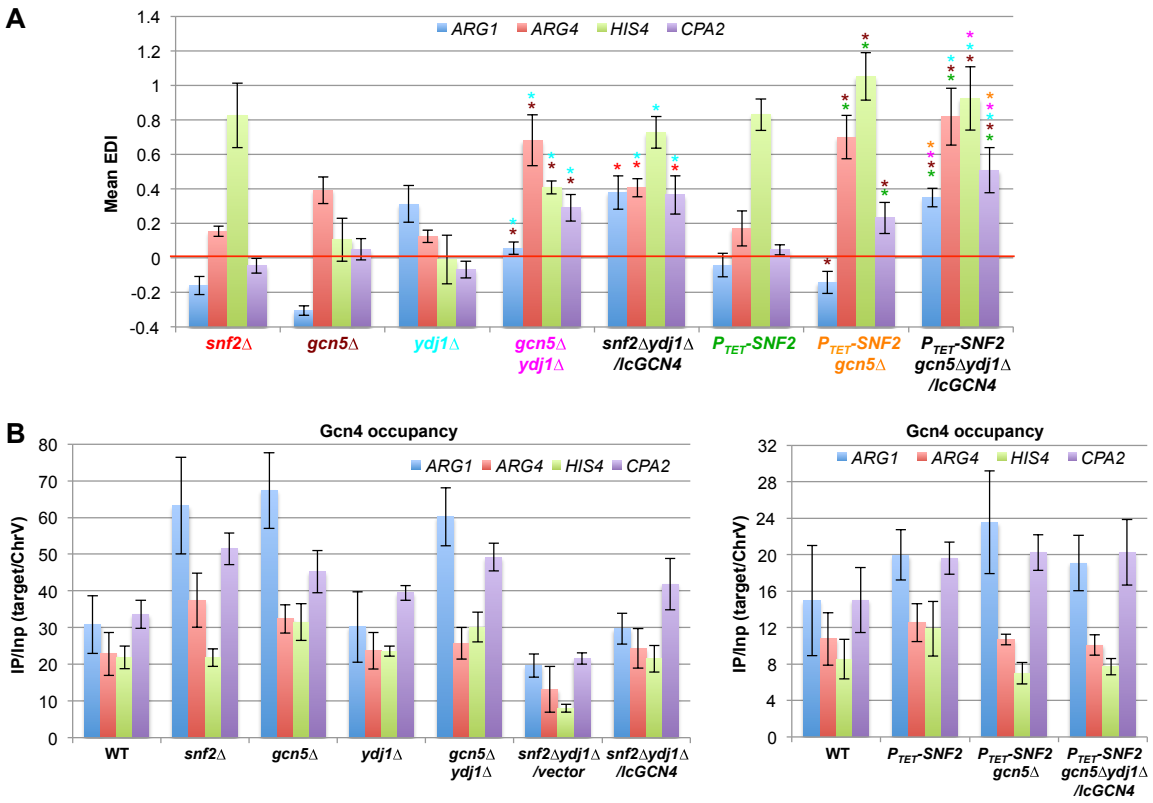

Supplemental Figure S4. Summary of conventional ChIP analysis of H3 at four canonical Gcn4 target genes in different mutants. (A) Mean EDI values (± SD) were calculated as in Fig. S3A from 3 or more biological replicates for each gene in 8 different mutants. Asterisks indicating significant differences in Student's *t*-tests ($p<0.05$) are color-coded to indicate the strains being compared; thus, the cyan asterisk above the *ARG1* bar for *gcn5*Δ*ydj1*Δ indicates a mean EDI significantly different than that indicated by the *ARG1* bar for the *ydj1*Δ strain (labeled cyan). (B) Measurements of Gcn4 occupancies in the panel of mutants analyzed in (A) (plus the *snf2*Δ*ydj1*Δ/vector strain presented for comparison) with mean (±SD) values calculated from 3 biological replicates.

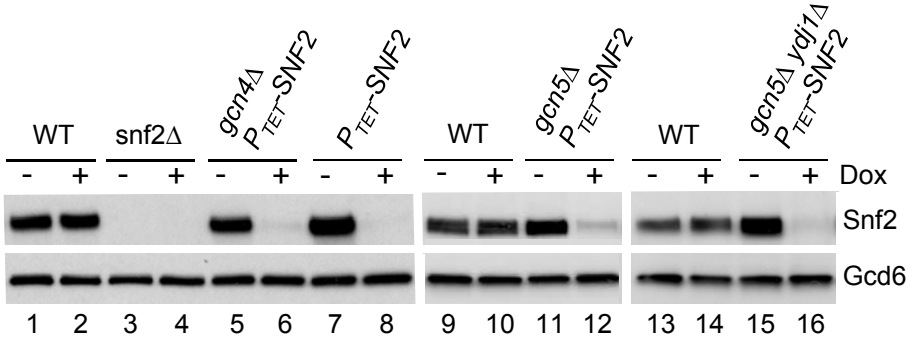

Supplemental Figure S5. Efficient doxycycline-mediated repression of Snf2 expressed from P_{TET}-*SNF2* in different mutants. Strains of the indicated genotypes cultured in SC medium were treated (+) or left untreated (-) with 10μg/mL doxycycline for 8h and subjected to Western analysis with antibodies against Snf2 or Gcd6 (analyzed as loading control).

A

		H3 EDI				Gcn4 occupancy (%WT)			
	Mutant	*ARG1*	*ARG4*	*HIS4*	*CPA2*	*ARG1*	*ARG4*	*HIS4*	*CPA2*
1	*snf2Δ*	-0.16	0.15	0.83	-0.05	2.1	1.6	1.0	1.5
2	*snf2Δ asf1Δ*	0	0.27	0.88	0.25	1.2	0.7	0.41	0.86
3	*asf1Δ snf2Δ/Ic Gcn4*	0.07	0.32	0.81	0.2	1.2	0.67	0.68	0.7
4	*snf2Δ yta7Δ*	0.11	0.38	0.92	0.27	1.2	0.59	0.36	0.76
5	*gcn5Δ*	-0.31	0.39	0.11	0.05	2.2	1.4	1.4	1.3
6	*gcn5Δ yta7Δ*	0	0.54	0.56	0.22	0.74	0.33	0.36	0.6
7	*gcn5Δ yta7Δ/Ic GCN4*	0.09	0.66	0.57	0.26	0.83	0.55	0.67	0.65

< 0	0-0.14	0.15-0.39	0.40-0.54	0.55-0.69	0.70-0.84	>0.84

B

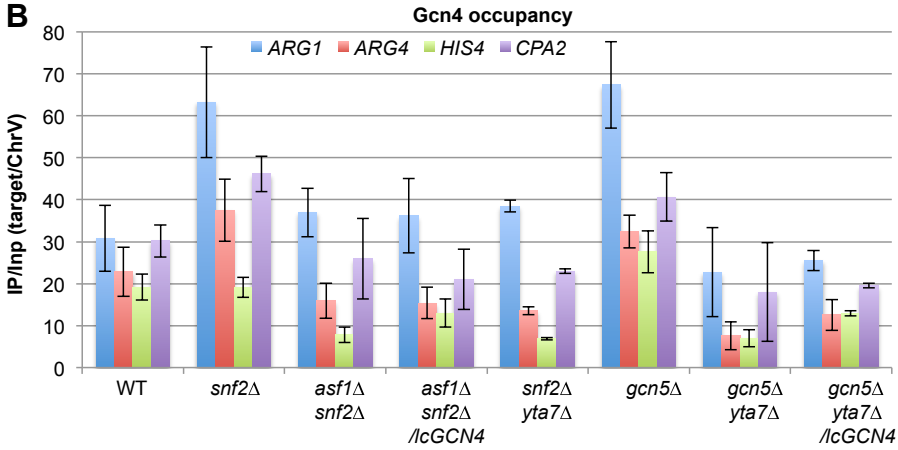

Supplemental Figure S6. Summary of conventional ChIP analysis of H3 and Gcn4 occupancies at four canonical Gcn4 target genes in different mutants. (A) Summary of EDI values and Gcn4 occupancies for the four genes in the indicated mutants, calculated and displayed as in Fig. S3A. (B) Measurements of Gcn4 occupancies for mutants analyzed in (A) with mean (± SD) values calculated from 3 biological replicates.

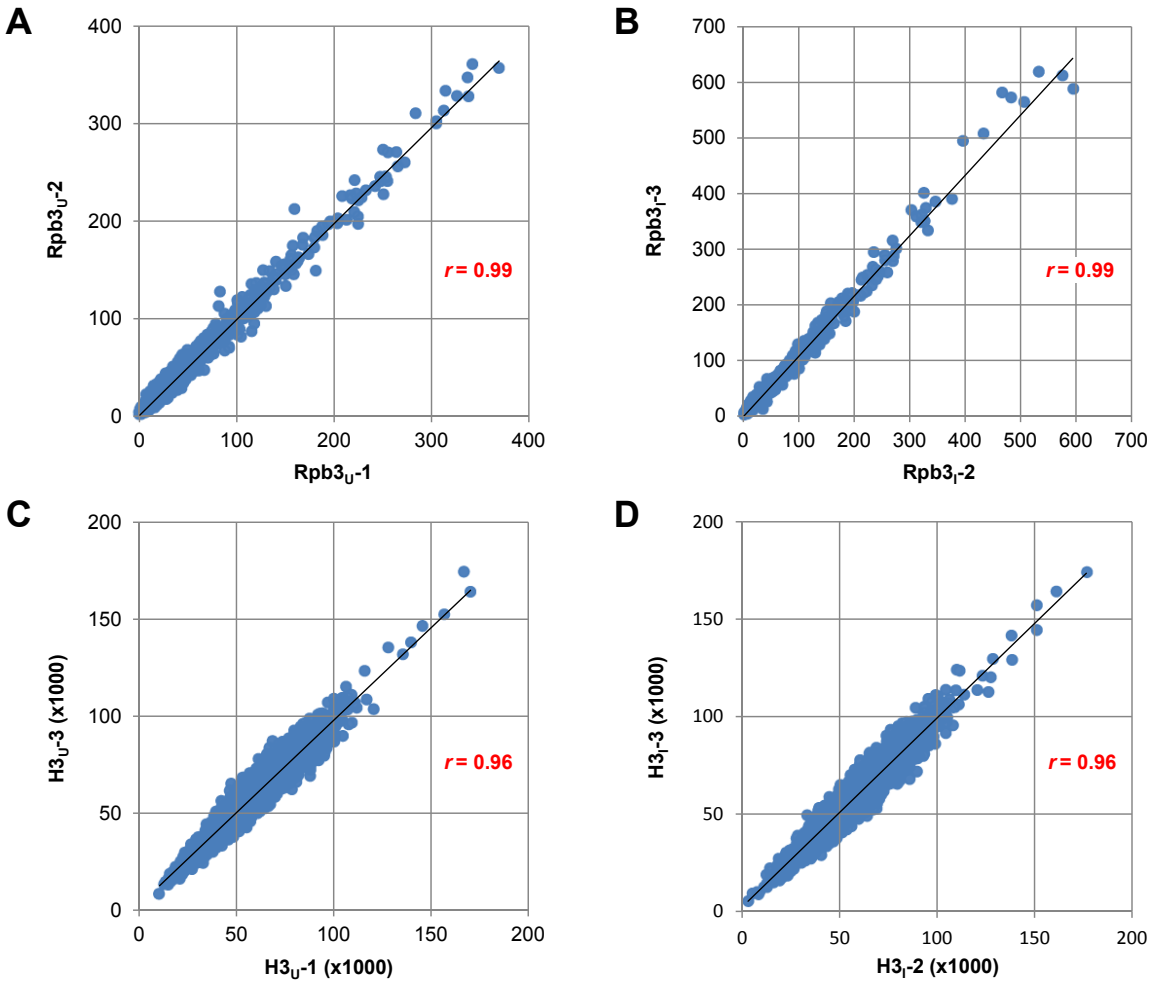

Supplemental Figure S7. H3 or Rpb3 densities in biological replicate experiments are highly correlated. Scatterplots are profiles of Rpb3 reads averaged over the CDS for each gene (A-B) or H3 reads in the 450 bp spanning nucleotides -389 to +61 (relative to the ATG codon) for each gene (C-D) calculated from ChIP-seq data in replicate experiments designated -1, -2, or -3, with the Pearson's correlations coefficient indicated. For Rpb3, reads were obtained from sequenced fragments of 50-150 bp for 5783 genes, with 6 genes (A) and 1 gene (B) excluded as their extremely large read numbers would compress most of the data points into a small sector of the plots. H3 reads were obtained from sequenced fragments of 50-300 bp for 5783 genes, with 5 genes excluded from both plots (C-D) due to their extremely large read numbers.

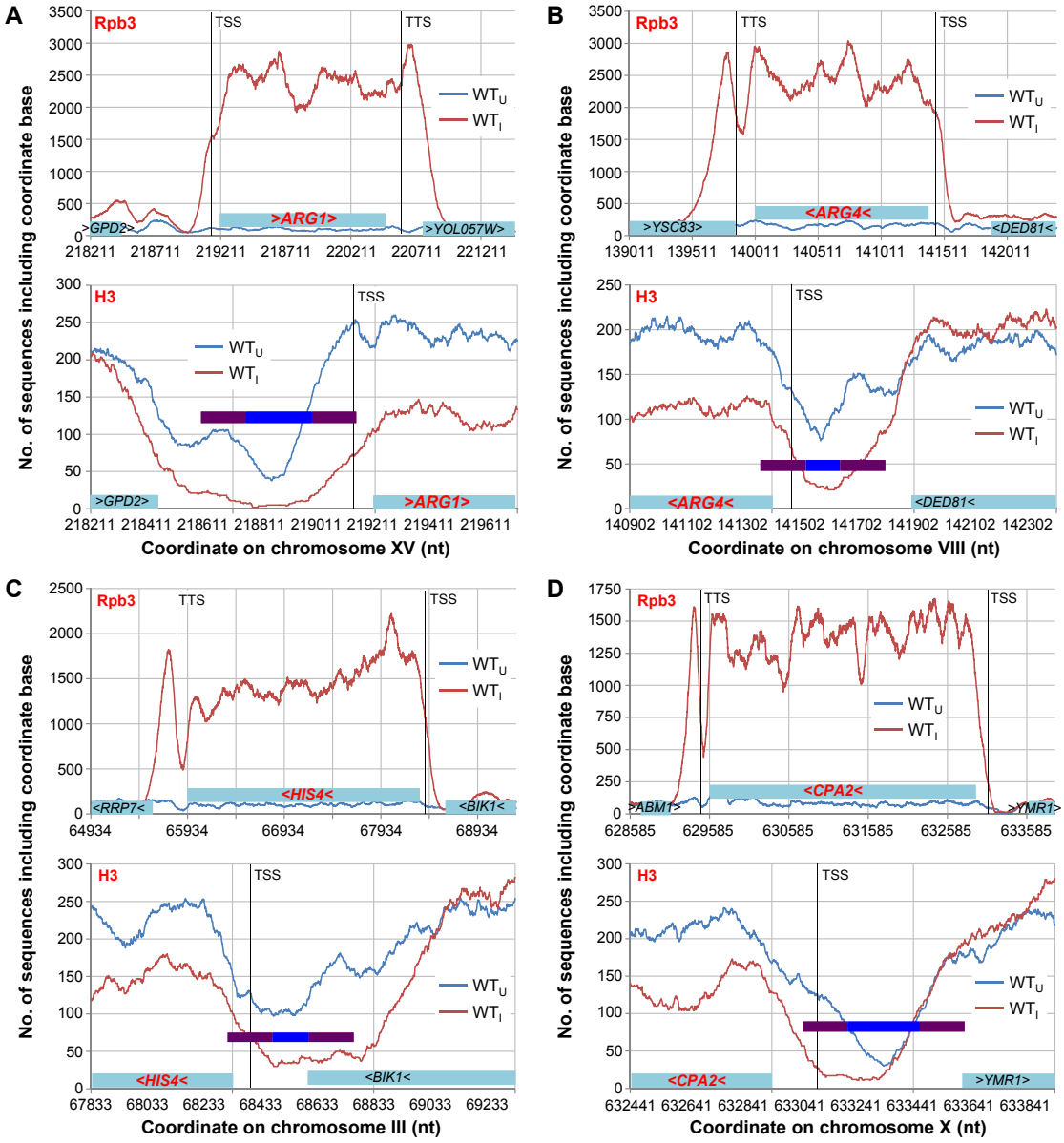

Supplemental Figure S8. SM-induction evokes high-level Rpb3 in CDS and depletion of H3 in promoters and CDS at four canonical Gcn4 target genes. Reads at each coordinate base of Rpb3 (upper panels) and H3 (lower panels) for the indicated chromosomal regions containing *ARG1* (A), *ARG4* (B), *HIS4* (C), and *CPA2* (D), determined from the average of ChIP-seq data from 3 biological replicates. Note different scales on the x-axis chosen to display the entire CDS for Rpb3 (upper plots) or zoom in on promoters for H3 occupancies (lower plots). TSS and TTS positions were taken from (Xu et al. 2009). Violet-blue-violet bars in H3 profiles represent annotated -1, NDR and +1 regions as determined in Fig. S10B.

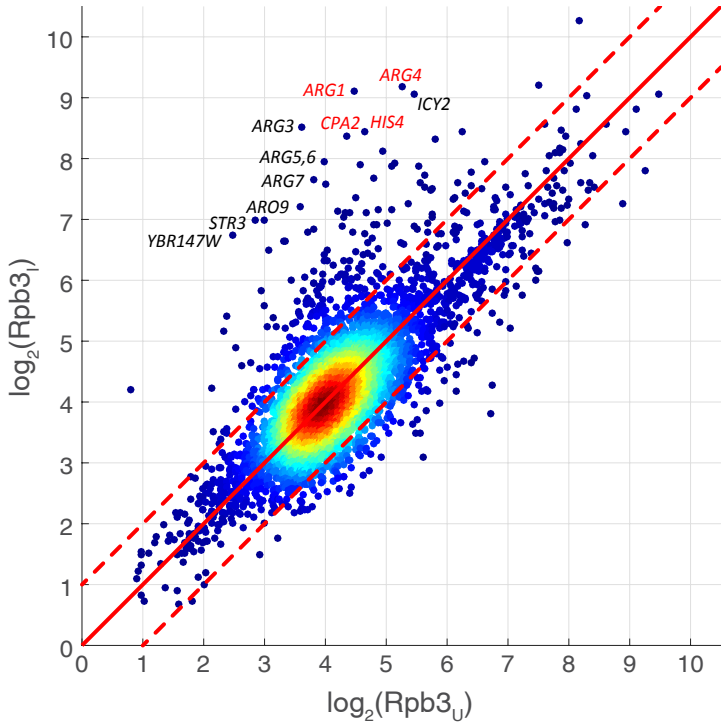

Supplemental Figure S9. Identification of genes exhibiting increased Rpb3 occupancies in CDS on SM-induction. Density plot of average Rpb3 occupancies per bp in CDS calculated from the average of ChIP-seq data from 3 biological replicates for SM-induced ($Rpb3_I$) or uninduced ($Rpb3_U$) WT cells. Individual genes are marked by blue filled circles; the coloring indicates increased density of genes (red is maximum). Dashed lines indicate differences of $\geq$2-fold. The four Gcn4 targets analyzed by conventional ChIP, *ARG1*, *ARG4*, *HIS4*, and *CPA2*, were among the genes displaying the largest Rpb3 induction ratios and induced levels of Rpb3 occupancy.

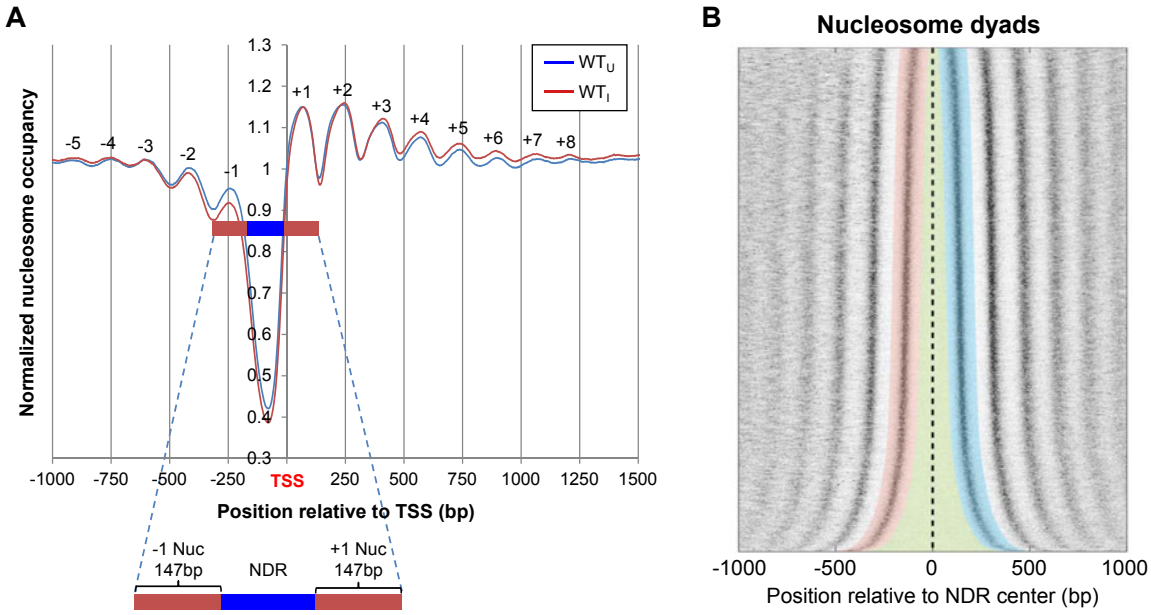

Supplemental Figure S10. Nuc-seq analysis of WT cells identifies consensus positions of the -1 nucleosome, NDR, and +1 nucleosomes and locations of these regions at each gene. Paired-end sequencing of mononucleosome core particles prepared by MNase digestion of nuclei was conducted for SM-induced or uninduced WT cells, averaging results from 2 biological replicates for each condition. (A) TSS plots for all genes showing consensus locations of -1, NDR, and +1 regions. (B) Nucleosome densities for all genes sorted by NDR length and aligned relative to the NDR centers (dotted line), with each row giving results for a single gene. Pink and cyan zones demarcate 147bp surrounding the dyads of the -1 and +1 nucleosomes, respectively, and the intervening NDRs are in lime green.

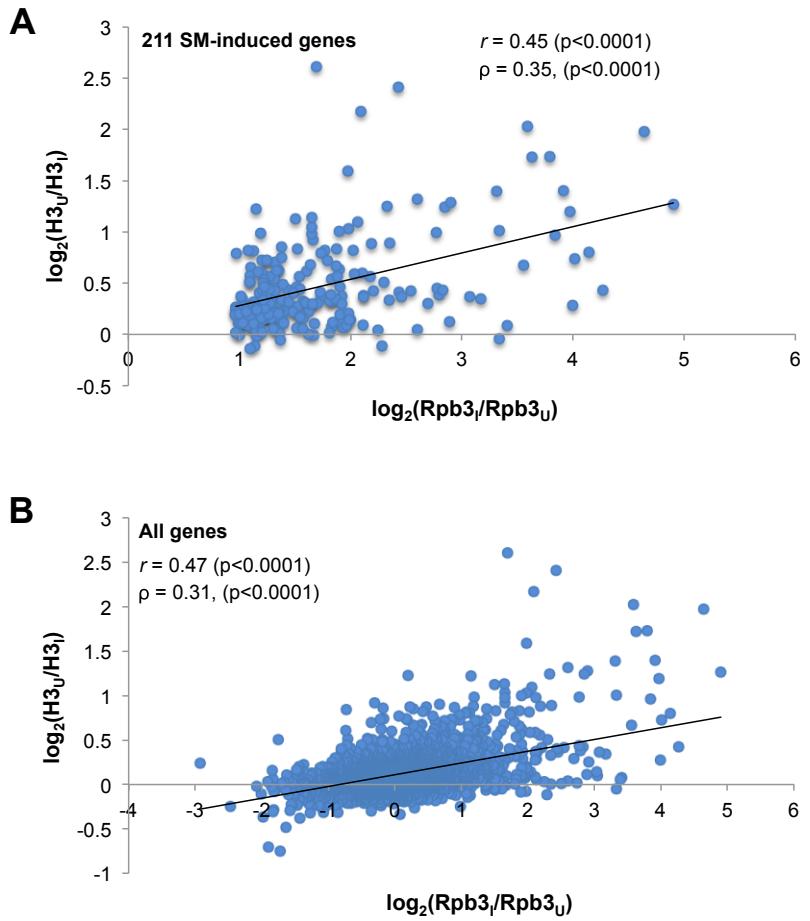

Supplemental Figure S11. Promoter depletion of H3 in SM-induced cells is correlated with changes in Rpb3 occupancies for 211 induced genes and for all genes. (A) The ratio of relative H3 occupancies per bp in the [-1,NDR,+1] windows defined in Fig. S10B in WT_U versus WT_I cells plotted against the ratio of Rpb3 occupancies per bp in CDS in WT_I versus WT_U cells, for the set of 211 SM-induced genes (defined in RESULTS), calculated from the average of ChIP-seq data from 3 biological replicates. Pearson's (r) and Spearman's (ρ) correlation coefficients are indicated. (B) Same as (A) except for all genes.

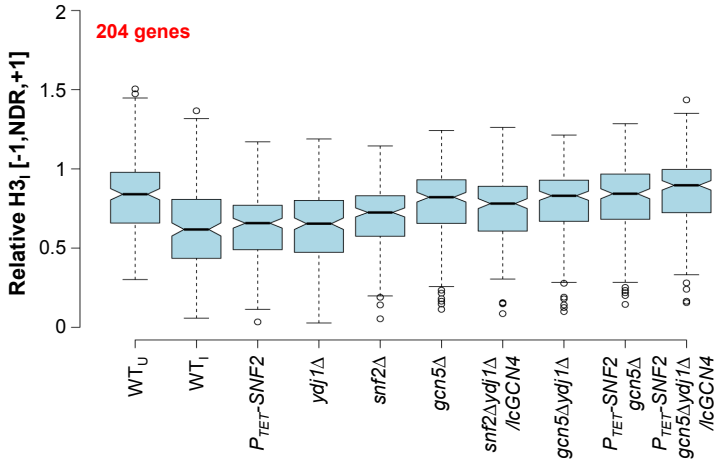

Supplemental Figure S12. Elimination of Snf2, Ydj1, or Gcn5 elevates H3 occupancies at highly induced genes. Notched box-plots of relative H3 occupancies per bp in the [-1,NDR,+1] window under inducing conditions for the 204 highly induced genes.

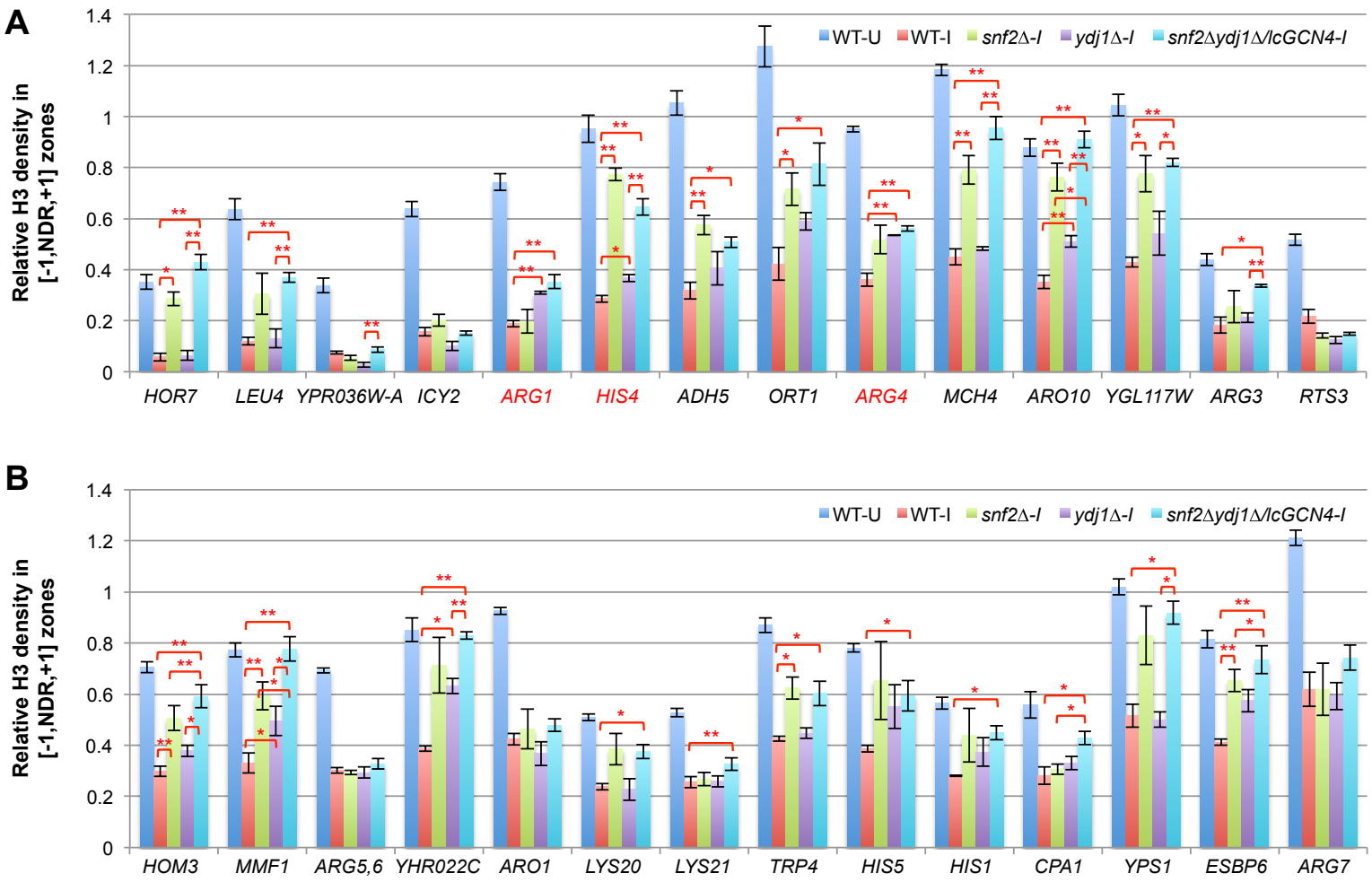

Supplemental Figure S13. Continued on next page.

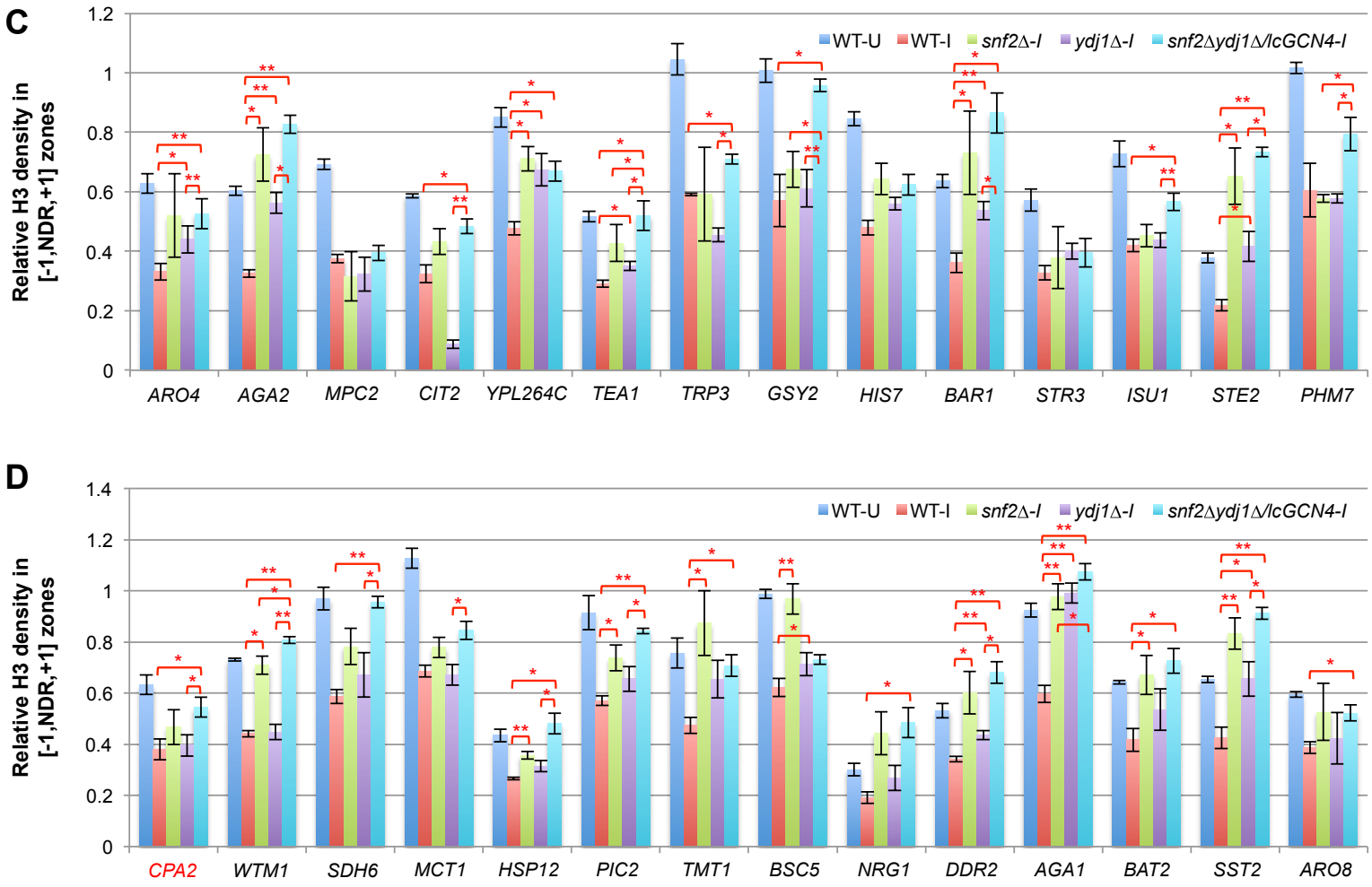

Supplemental Figure S13. Continued on next page.

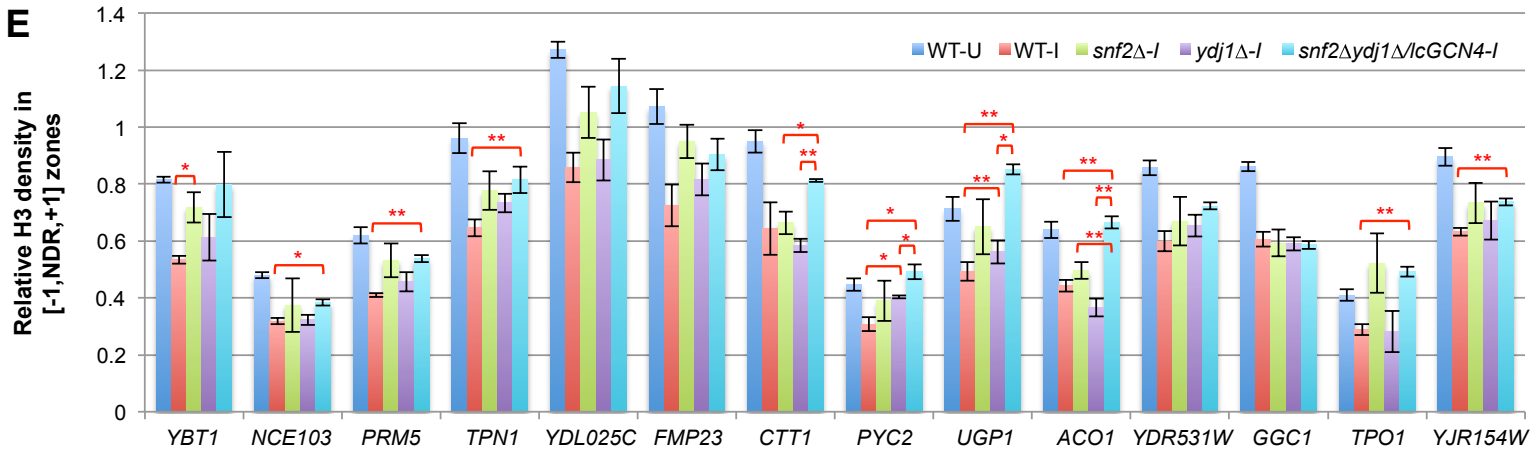

Supplemental Figure S13. Effects of *snf2*Δ and *ydj1*Δ single or double mutations on promoter H3 occupancies of 70 SM-induced exemplar genes. (A-E) Mean (± SD) relative H3 occupancies per bp in the [-1,NDR,+1] regions determined by ChIP-seq analysis for each of three biological replicates for WT under inducing and uninducing conditions, and mutant strains under SM-inducing conditions. Asterisks indicate significant differences in Student's *t*-tests: *, $p<0.05$; **, $p<0.01$. Genes are listed in descending order of H3 eviction in WT cells, quantified as WT_U/WT_I.

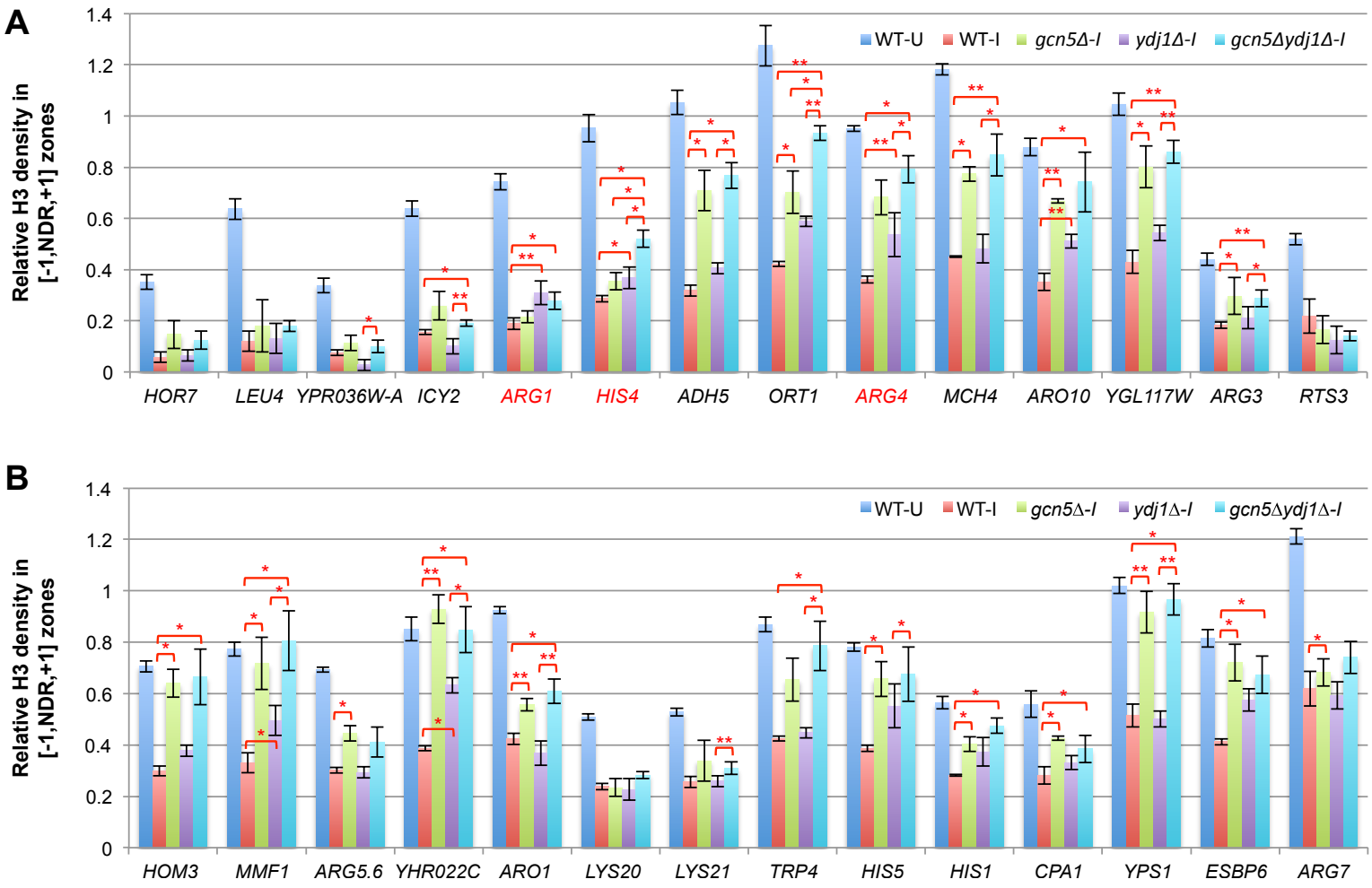

Supplemental Figure S14. Continued on next page.

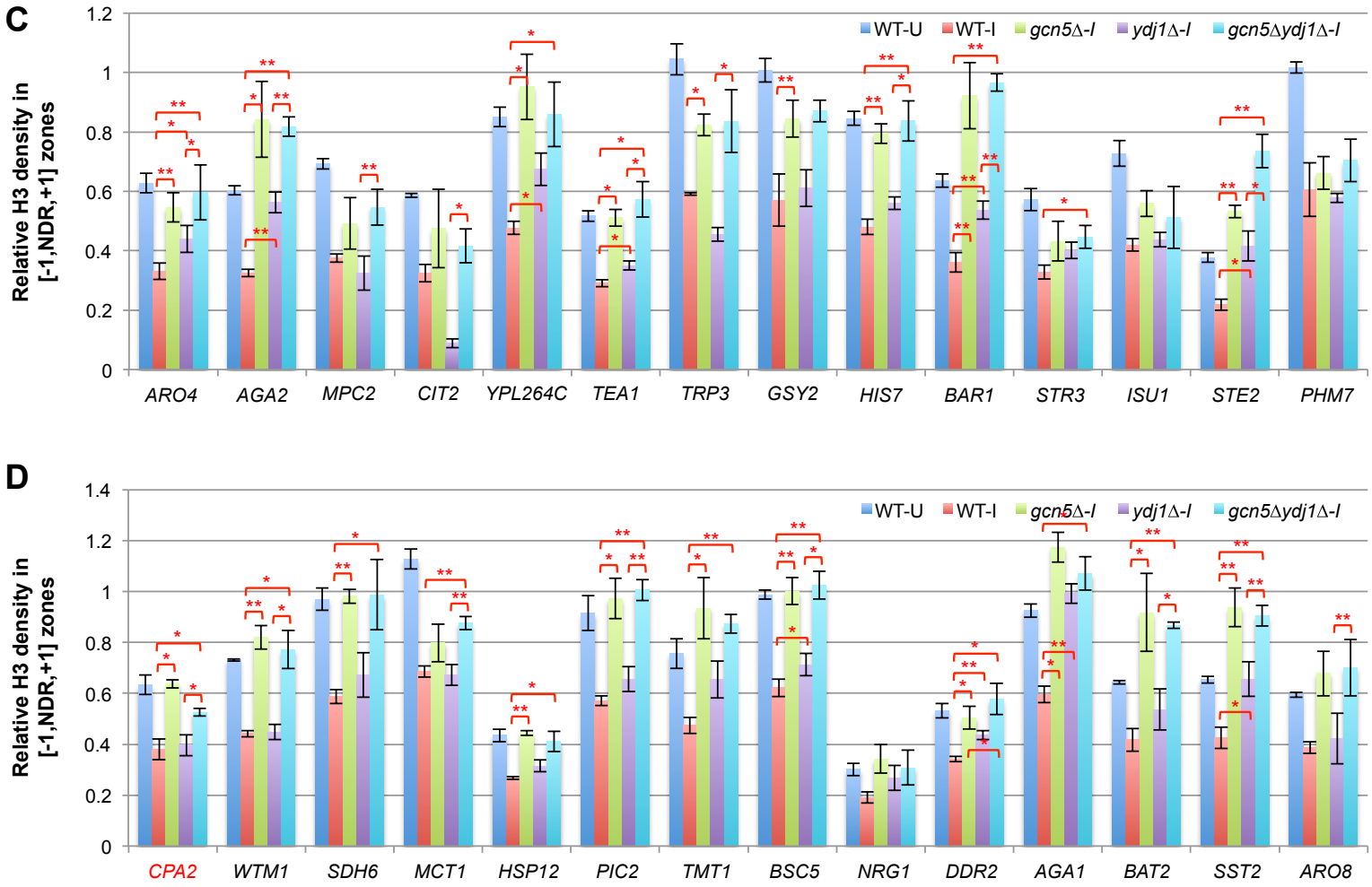

Supplemental Figure S14. Continued on next page.

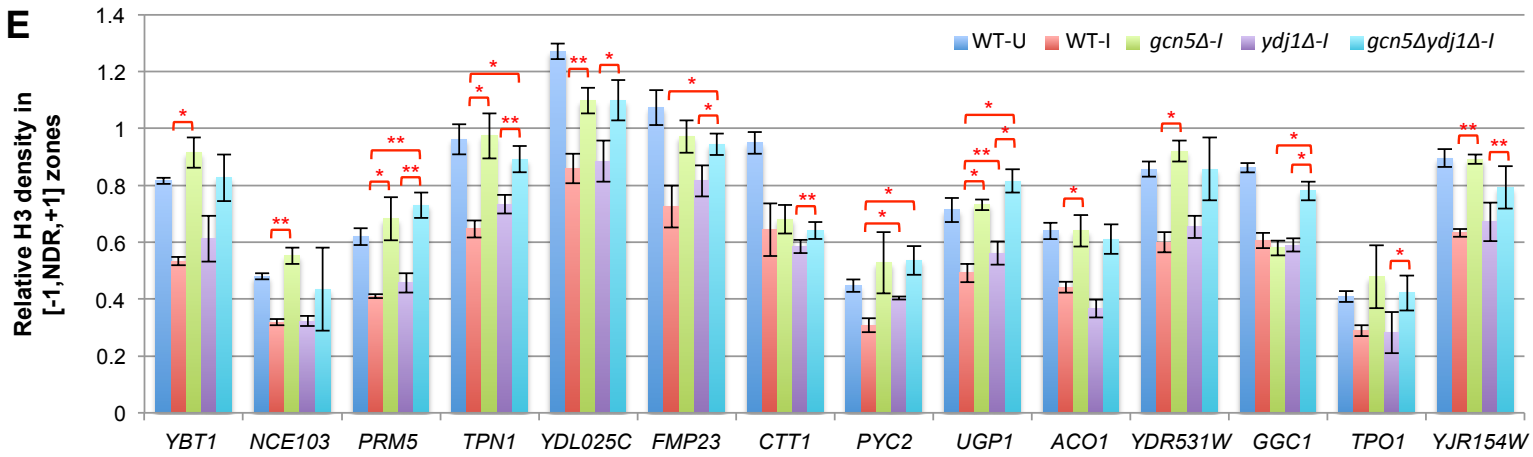

Supplemental Figure S14. Effects of *gcn5*Δ and *ydj1*Δ single or double mutations on promoter H3 occupancies of 70 SM-induced exemplar genes. (A-E) Mean (± SD) relative H3 occupancies per bp in the [-1,NDR,+1] regions determined by ChIP-seq analysis for each of three biological replicates for WT under both inducing and uninducing conditions, and mutant strains under SM-inducing conditions. Asterisks indicate significant differences in Student's *t*-tests: *, $p<0.05$; **, $p<0.01$. Genes are listed in descending order of H3 eviction in WT cells, quantified as WT_U/WT_I. Results for WT and *ydj1*Δ are re-plotted from Fig. S13 for comparison.

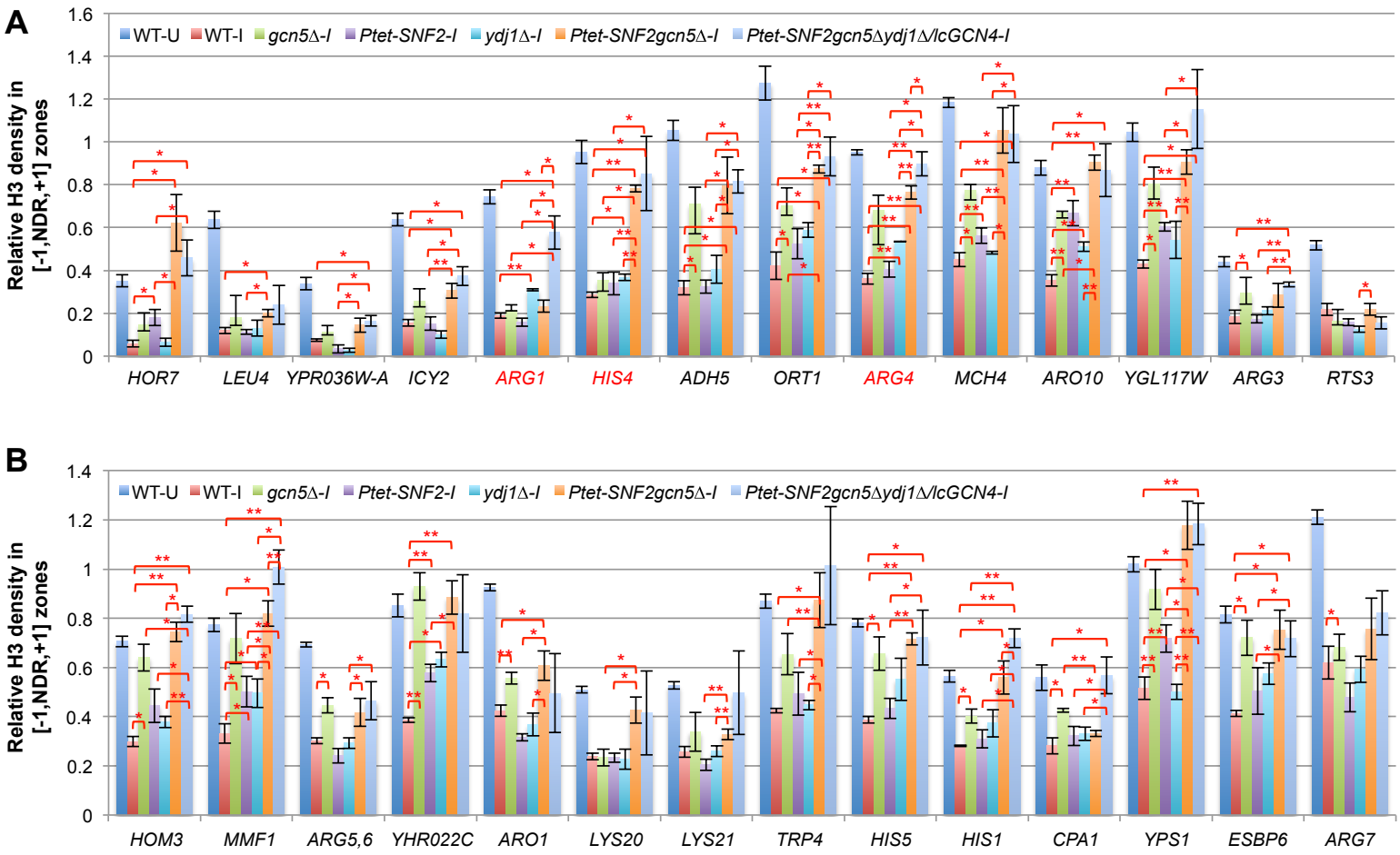

Supplemental Figure S15. Continued on next page.

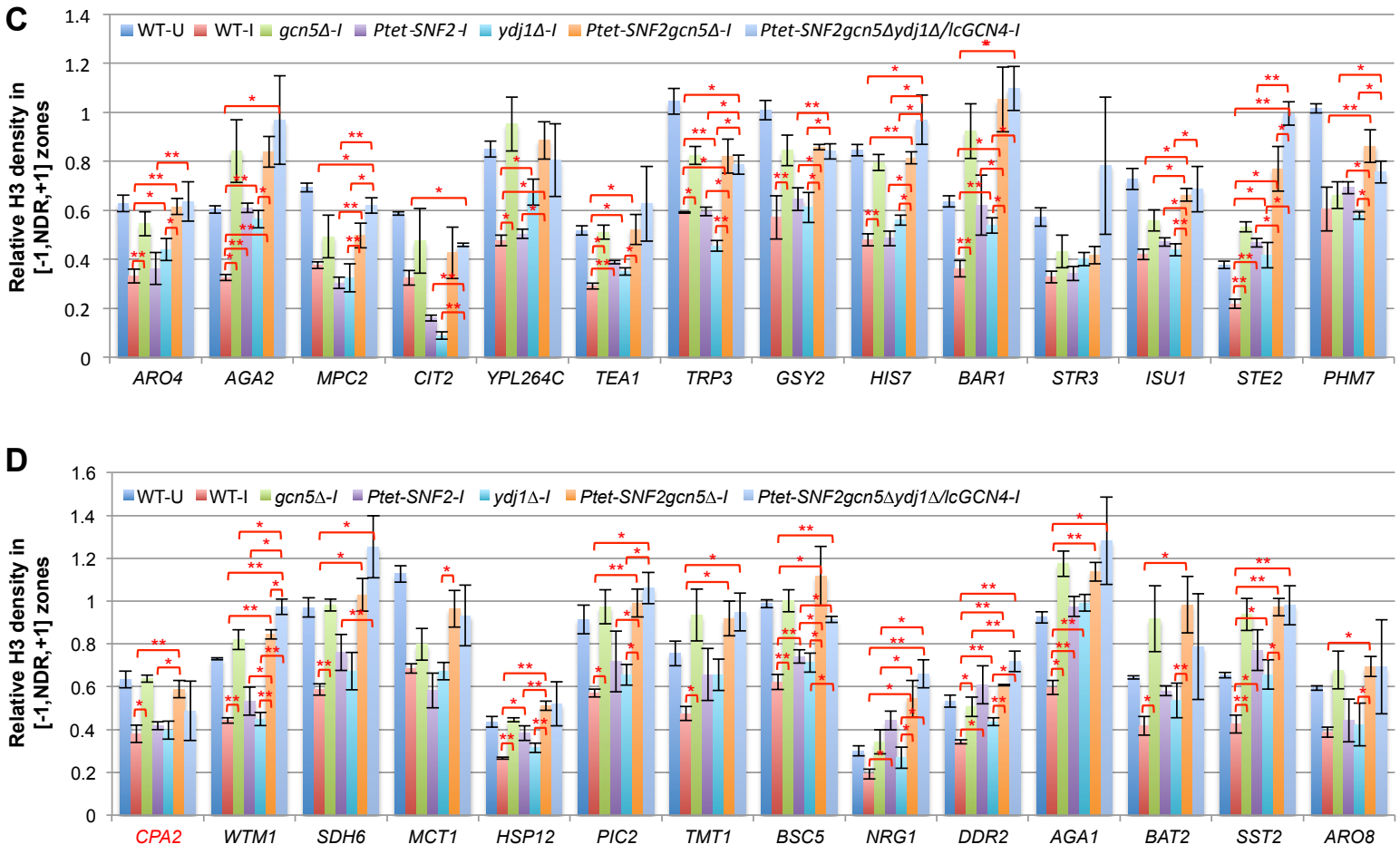

Supplemental Figure S15. Continued on next page.

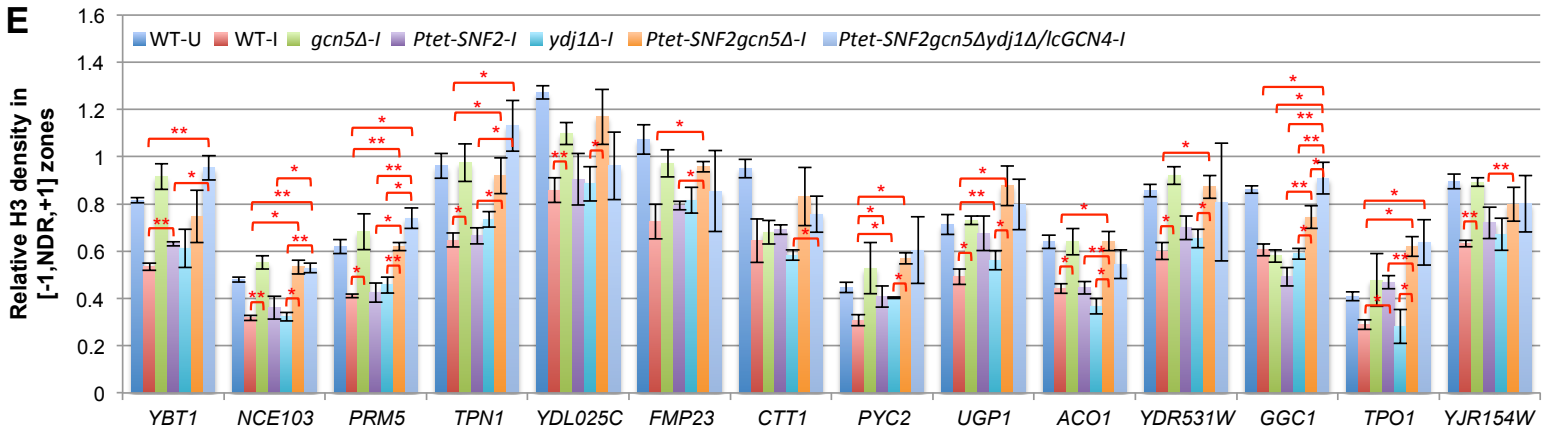

Supplemental Figure S15. Effects of *gcn5*Δ, P_{TET}-*SNF2*, *ydj1*Δ, P_{TET}-*SNF2 gcn5*Δ, and P_{TET}-*SNF2 gcn5*Δ *ydj1*Δ/lcGCN4 single, double or triple mutations on promoter H3 occupancies of 70 SM-induced exemplar genes. (A-E) Mean (± SD) relative H3 occupancies per bp in the [-1,NDR,+1] regions determined by ChIP-seq analysis for each of three biological replicates for WT under both inducing and uninducing conditions, and mutant strains under SM-inducing conditions . Asterisks indicate significant differences in Student's *t*-tests: *, $p<0.05$; **, $p<0.01$. Genes are listed in descending order of H3 eviction in WT cells, quantified as WT_U/WT_I. Results for WT, *gcn5*Δ and *ydj1*Δ are re-plotted from Fig. S14 for comparison.

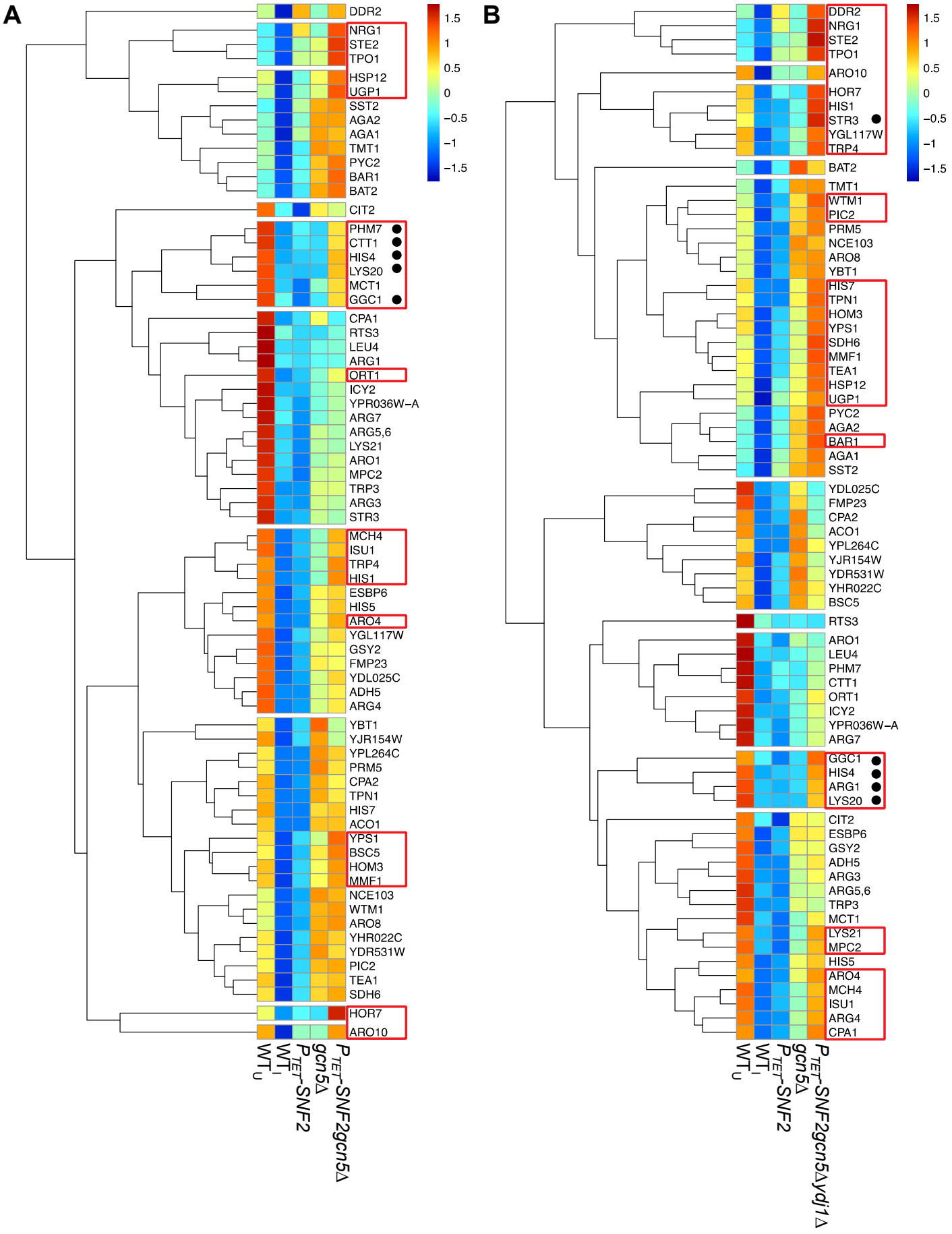

Supplemental Figure S16. Caption on next page.

Supplemental Figure S16. Snf2, Gcn5, and Ydj1 cooperate in promoter H3 eviction at many of the 70 exemplar induced genes. (A-B) Cluster analysis of changes in relative H3 occupancies per bp in the [-1,NDR,+1] regions for the 70 exemplar genes in single, double and triple mutants. Relative H3 densities for each gene in the appropriate mutants shown in Fig. S15 were averaged and z-scores calculated for the results for each mutant. Hierarchical clustering analysis of the average relative H3 occupancies in the [-1,NDR,+1] regions was performed as described in Fig. 4A-B. Boxed genes display additive effects of mutations; those with bullets show strong eviction defects only in double mutants.

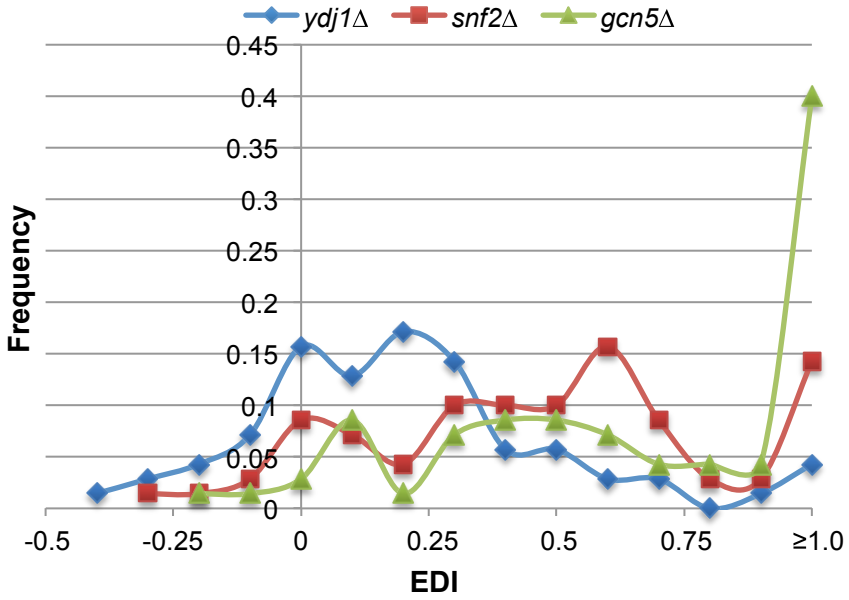

Supplemental Figure S17. Distribution of histone eviction defect indices for the 70 exemplar SM-induced genes in single mutants lacking Snf2, Ydj1, or Gcn5. The proportions of the 70 exemplar genes exhibiting EDI values falling into different bins is plotted for each mutant using the mean EDI values from Supplementary file S5, sheet 2. EDI was calculated as the increase in H3 occupancy in the mutant normalized to the difference in occupancy between uninduced and induced WT cells.

	Gene	WT-I vs snf2Δ-I	ydj1Δ vs snf2Δydj1Δ	WT-I vs Ptet-SNF2	gcn5Δ vs Ptet-SNF2gcn5Δ	gcn5Δydj1Δ vs Ptet-SNF2gcn5Δydj1Δ	**Total Snf2-dep**
1	*HOR7*	0.012	0.008	0.019	0.052	0.035	
2	*LEU4*	0.087	0.003	0.309	0.51	0.520	
3	*YPR036W-A*	0.043*	0.003	0.148	0.254	0.175	
4	*ICY2*	0.228	0.101	0.850	0.212	0.028	
5	*ARG1*	0.813	0.195	0.297	0.408	0.018	
6	*HIS4*	0.003	0.008	0.246	0.012	0.150	
7	*ADH5*	0.00015	0.227	0.701	0.146	0.540	
8	*ORT1*	0.022	0.107	0.360	0.048	0.978	
9	*ARG4*	0.089	0.068	0.410	0.605	0.301	
10	*MCH4*	0.003	0.005	0.003	0.082	0.090	
11	*ARO10*	0.003	0.001	0.008	0.026	0.407	
12	*YGL117W*	0.029	0.044	0.004	0.312	0.205	
13	*ARG3*	0.137	0.010	0.591	0.809	0.119	
14	*RTS3*	0.064*	0.114	0.116	0.209	0.659	
15	*HOM3*	0.009	0.027	0.122	0.217	0.109	
16	*MMF1*	0.003	0.020	0.021	0.371	0.232	
17	*ARG5,6*	0.542	0.317	0.111	0.543	0.098	
18	*YHR022C*	0.06	0.009	0.009	0.663	0.882	
19	*ARO1*	0.421	0.089	0.026*	0.309	0.516	
20	*LYS20*	0.07	0.087	0.853	0.029	0.417	
21	*LYS21*	0.669	0.118	0.054*	0.842	0.294	
22	*TRP4*	0.031	0.083	0.398	0.008	0.462	
23	*HIS5*	0.127	0.173	0.209	0.407	0.791	
24	*HIS1*	0.161	0.147	0.391	0.052	0.023	
25	*CPA1*	0.235	0.107	0.174	0.004*	0.021	
26	*YPS1*	0.067	0.013	0.002	0.157	0.009	
27	*ESBP6*	0.01	0.136	0.337	0.794	0.287	
28	*ARG7*	0.987	0.163	0.031*	0.308	0.523	
29	*ARO4*	0.161	0.004	0.673	0.111	0.784	
30	*AGA2*	0.019	0.025	0.001	0.971	0.340	
31	*MPC2*	0.453	0.303	0.105	0.88	0.297	
32	*CIT2*	0.163	0.004	0.026*	0.25	0.440	
33	*YPL264C*	0.034	0.927	0.274	0.31	0.596	
34	*TEA1*	0.064	0.021	0.002	0.883	0.732	
35	*TRP3*	0.994	0.011	0.683	0.97	0.672	
36	*GSY2*	0.28	0.010	0.515	0.818	0.520	
37	*HIS7*	0.066	0.234	0.616	0.401	0.100	

WT-I vs ydj1Δ-I	snf2Δ vs snf2Δydj1Δ	gcn5Δ vs gcn5Δydj1Δ	Ptet-SNF2gcn5Δ vs Ptet-SNF2gcn5Δydj1Δ	**Total Ydj1-dep**
0.813	0.069	0.526	0.085*	
0.722	0.278	0.976	0.537	
0.034*	0.118	0.234	0.426	
0.027*	0.053*	0.12	0.21	
0.008	0.087	0.103	0.011	
0.013	0.084*	0.047	0.645	
0.099	0.2	0.661	0.897	
0.07	0.409	0.043	0.4016	
0.009	0.448	0.295	0.049	
0.364	0.084	0.487	0.575	
0.004	0.019	0.429	0.713	
0.211	0.419	0.351	0.28	
0.082	0.221	0.658	0.346	
0.058*	0.523	0.469	0.059*	
0.069	0.009	0.713	0.093	
0.013	0.031	0.222	0.007	
0.58	0.247	0.278	0.232	
0.013	0.275	0.235	0.489	
0.12	0.844	0.099	0.54	
0.7	0.888	0.282	0.91	
0.882	0.179	0.567	0.329	
0.114	0.644	0.192	0.566	
0.104	0.462	0.745	0.951	
0.133	0.873	0.199	0.019	
0.125	0.013	0.335	0.051	
0.717	0.471	0.587	0.936	
0.054	0.012	0.119	0.735	
0.278	0.361	0.221	0.684	
0.0133	0.956	0.279	0.816	
0.008	0.295	0.81	0.365	
0.401	0.347	0.111	0.103	
0.003*	0.323	0.386	0.715	
0.047	0.054*	0.019	0.317	
0.017	0.044	0.286	0.29	
0.009*	0.439	0.901	0.65	
0.582	0.016	0.709	0.418	
0.069	0.435	0.282	0.19	

WT-I vs gcn5Δ-I	ydj1Δ vs gcn5Δydj1Δ	Ptet-SNF2 vs Ptet-SNF2gcn5Δ	**Total Gcn5-dep**
0.105	0.164	0.03	
0.079	0.051	0.042	
0.118	0.037	0.033	
0.083	0.002	0.006	
0.129	0.284	0.098	
0.205	0.031	0.007	
0.035	0.023	0.022	
0.039	0.002	0.011	
0.118	0.021	0.008	
0.023	0.028	0.011	
0.0001	0.107	0.07	
0.026	0.010	0.021	
0.019	0.018	0.138	
0.248	0.437	0.193	
0.012	0.056	0.059	
0.013	0.043	0.025	
0.032	0.056	0.091	
0.006	0.036	0.026	
0.008	0.000	0.024	
0.883	0.114	0.022	
0.232	0.002	0.007	
0.072	0.046	0.023	
0.023	0.030	0.002	
0.025	0.228	0.077	
0.02	0.254	0.808	
0.004	0.002	0.041	
0.028	0.172	0.046	
0.026	0.070	0.067	
0.005	0.045	0.068	
0.025	0.008	0.059	
0.237	0.000	0.01	
0.32	0.022	0.064	
0.032	0.234	0.011	
0.016	0.022	0.076	
0.014	0.028	0.027	
0.006	0.065	0.014	
0.006	0.041	0.012	

Supplemental Figure S18. Continued on next page.

	Gene	WT-I vs snf2Δ-I	ydj1Δ vs snf2Δydj1Δ	WT-I vs Ptet-SNF2	gcn5Δ vs Ptet-SNF2gcn5Δ	gcn5Δydj1Δ vs Ptet-SNF2gcn5Δydj1Δ	**Total Snf2-dep**	WT-I vs ydj1Δ-I	snf2Δ vs snf2Δydj1Δ	gcn5Δ vs gcn5Δydj1Δ	Ptet-SNF2gcn5Δ vs Ptet-SNF2gcn5Δydj1Δ	**Total Ydj1-dep**	WT-I vs gcn5Δ-I	ydj1Δ vs gcn5Δydj1Δ	Ptet-SNF2 vs Ptet-SNF2gcn5Δ	**Total Gcn5-dep**
38	*BAR1*	0.047	0.025	0.062	0.186	0.106		0.009	0.455	0.66	0.798		0.0096	0.003	0.050	
39	*STR3*	0.564	0.740	0.726	0.827	0.211		0.125	0.733	0.812	0.240		0.202	0.284	0.143	
40	*ISU1*	0.347	0.003	0.171	0.014	0.330		0.596	0.124	0.698	0.672		0.08	0.497	0.016	
41	*STE2*	0.02	0.011	0.007	0.075	0.063		0.02	0.31	0.062	0.023		0.005	0.023	0.048	
42	*PHM7*	0.678	0.022	0.261	0.138	0.588		0.73	0.047	0.651	0.311		0.637	0.173	0.043	
43	*CPA2*	0.347	0.024	0.272	0.317	0.754		0.798	0.177	0.005*	0.454		0.023	0.024	0.029	
44	*WTM1*	0.014	0.002	0.162	0.595	0.026		0.822	0.035	0.489	0.028		0.007	0.040	0.012	
45	*SDH6*	0.061	0.028	0.058	0.488	0.004		0.379	0.077	0.949	0.200		0.00009	0.140	0.097	
46	*MCT1*	0.087	0.031	0.145	0.167	0.679		0.714	0.29	0.165	0.825		0.115	0.006	0.052	
47	*HSP12*	0.005	0.031	0.044	0.088	0.390		0.104	0.084	0.281	0.894		0.0007	0.109	0.008	
48	*PIC2*	0.023	0.034	0.249	0.311	0.464		0.058	0.092	0.348	0.382		0.015	0.005	0.048	
49	*TMT1*	0.05	0.315	0.135	0.919	0.485		0.106	0.124	0.431	0.083		0.027	0.053	0.099	
50	*BSC5*	0.003	0.643	0.011	0.205	0.144		0.04	0.048	0.006	0.190		0.006	0.025	0.038	
51	*NRG1*	0.068	0.084	0.033	0.028	0.057		0.166	0.718	0.267	0.227		0.052	0.122	0.360	
52	*DDR2*	0.051	0.012	0.046	0.078	0.004		0.004	0.131	0.086	0.080		0.043	0.064	0.990	
53	*AGA1*	0.004	0.059	0.006	0.157	0.375		0.0045	0.034	0.259	0.424		0.012	0.385	0.071	
54	*BAT2*	0.013	0.064	0.069	0.471	0.687		0.118	0.475	0.672	0.530		0.023	0.028	0.066	
55	*SST2*	0.001	0.030	0.034	0.714	0.427		0.012	0.236	0.568	0.936		0.003	0.007	0.084	
56	*ARO8*	0.283	0.324	0.565	0.732	0.979		0.719	0.962	0.659	0.994		0.061	0.003	0.052	
57	*YBT1*	0.044	0.070	0.007	0.227	0.283		0.328	0.245	0.262	0.141		0.013	0.096	0.304	
58	*NCE103*	0.438	0.085	0.252	0.682	0.471		0.706	0.915	0.393	0.905		0.009	0.377	0.074	
59	*PRM5*	0.088	0.132	0.667	0.273	0.888		0.169	0.917	0.183	0.110		0.031	0.010	0.033	
60	*TPN1*	0.122	0.212	0.635	0.101*	0.141		0.123	0.587	0.38	0.224		0.011	0.004	0.042	
61	*YDL025C*	0.063	0.141	0.683	0.391	0.421		0.673	0.549	0.982	0.375		0.006	0.041	0.238	
62	*FMP23*	0.058	0.310	0.392	0.808	0.586		0.059	0.618	0.643	0.487		0.07	0.018	0.027	
63	*CTT1*	0.849	0.003	0.502	0.176	0.075		0.52	0.032	0.426	0.290		0.554	0.008	0.217	
64	*PYC2*	0.316	0.038	0.019	0.628	0.646		0.029	0.087	0.884	0.761		0.126	0.067	0.078	
65	*UGP1*	0.092	0.018	0.103	0.169	0.802		0.009	0.132	0.086	0.572		0.021	0.041	0.212	
66	*ACO1*	0.146	0.003	0.892	0.837	0.0701*		0.037*	0.001	0.595	0.210		0.028	0.054	0.005	
77	*YDR531W*	0.48	0.131	0.190	0.301	0.862		0.401	0.407	0.349	0.772		0.025	0.073	0.121	
68	*GGC1*	0.826	0.841	0.123	0.088	0.072		0.658	0.794	0.042	0.034		0.007*	0.014	0.005	
69	*TPO1*	0.106	0.078	0.022	0.310	0.182		0.924	0.751	0.387	0.849		0.151	0.017	0.004	
70	*YJR154W*	0.168	0.234	0.145	0.155	0.961		0.478	0.935	0.148	0.979		0.0005	0.003	0.004	

	WT-I vs snf2Δ-I	ydj1Δ vs snf2Δydj1Δ	WT-I vs Ptet-SNF2	gcn5Δ vs Ptet-SNF2gcn5Δ	gcn5Δydj1Δ vs Ptet-SNF2gcn5Δydj1Δ	**Total Snf2-dep**	WT-I vs ydj1Δ-I	snf2Δ vs snf2Δydj1Δ	gcn5Δ vs gcn5Δydj1Δ	Ptet-SNF2gcn5Δ vs Ptet-SNF2gcn5Δydj1Δ	**Total Ydj1-dep**	WT-I vs gcn5Δ-I	ydj1Δ vs gcn5Δydj1Δ	Ptet-SNF2 vs Ptet-SNF2gcn5Δ	**Total Gcn5-dep**
p ≤ 0.01	11	15	11	1	3	32	8	2	1	1	12	17	17	12	36
p ≤ 0.05, >0.01	14	19	8	6	6	19	11	11	4	6	17	29	25	28	29
p < 0.05	25	34	19	7	9	51	19	13	5	7	29	46	42	40	65
p > 0.05	45	36	51	63	61	19	51	57	65	63	41	24	28	30	5
Total	70	70	70	70	70	70	70	70	70	70	70	70	70	70	70

Supplemental Figure S18. Summary of effects of single, double or triple mutations that eliminate or deplete Snf2, Ydj1, and Gcn5 on promoter H3 occupancies of 70 SM-induced exemplar genes. Compilation of p-values from Student's *t*-tests conducted on results shown in Figs. S13-S15. Asterisks and muted colors indicate gene/mutant combinations where H3 occupancies are reduced rather than elevated in the mutant, indicating defects in nucleosome replacement versus eviction. Dependence on Snf2 for nucleosome eviction is summarized for each gene in column 8 ("Total Snf2-dep") using colors indicated at the bottom signifying p-value ranges for the comparison yielding the most significant difference between strains containing or lacking *SNF2*, tabulated in the preceding 5 columns. Similar procedures were followed to tabulate dependence on Ydj1 (columns 9-13) or Gcn5 (columns 14-17) for nucleosome eviction. Totals for each column are listed at the bottom. Results in columns 8, 13, and 17 for p-values <0.05 (yellow/lime/blue), summarizing dependence on each co-factor, were used to construct the Venn diagram in Fig. 4C.

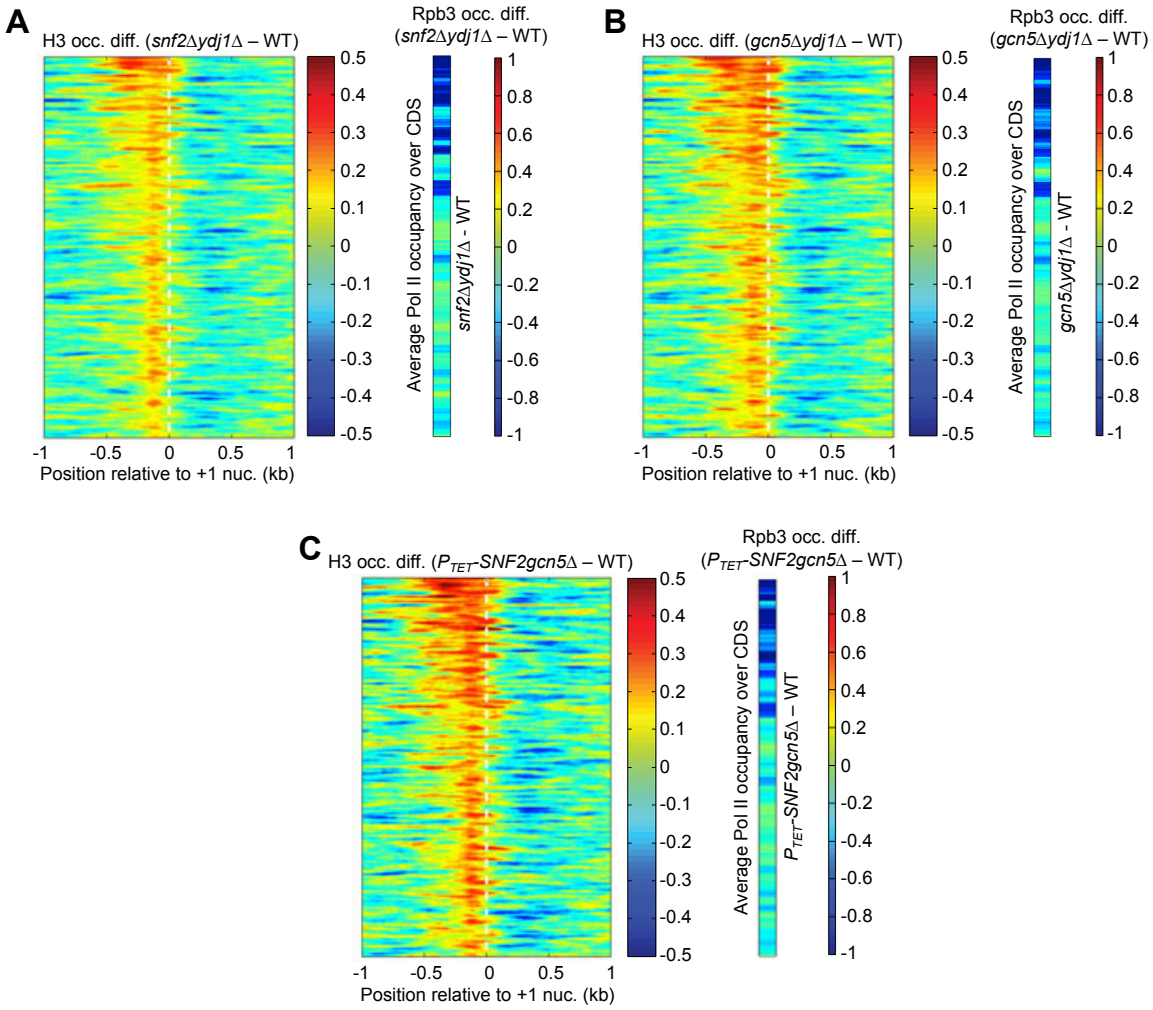

Supplemental Figure S19. Reductions in Pol II occupancy are associated with increased H3 promoter occupancy for 1000 genes with the greatest eviction of promoter nucleosomes in WT induced cells. (A-C) Heat maps for the identically-ordered 1000 genes shown in Fig. 2D, constructed as described there, for the indicated mutants.

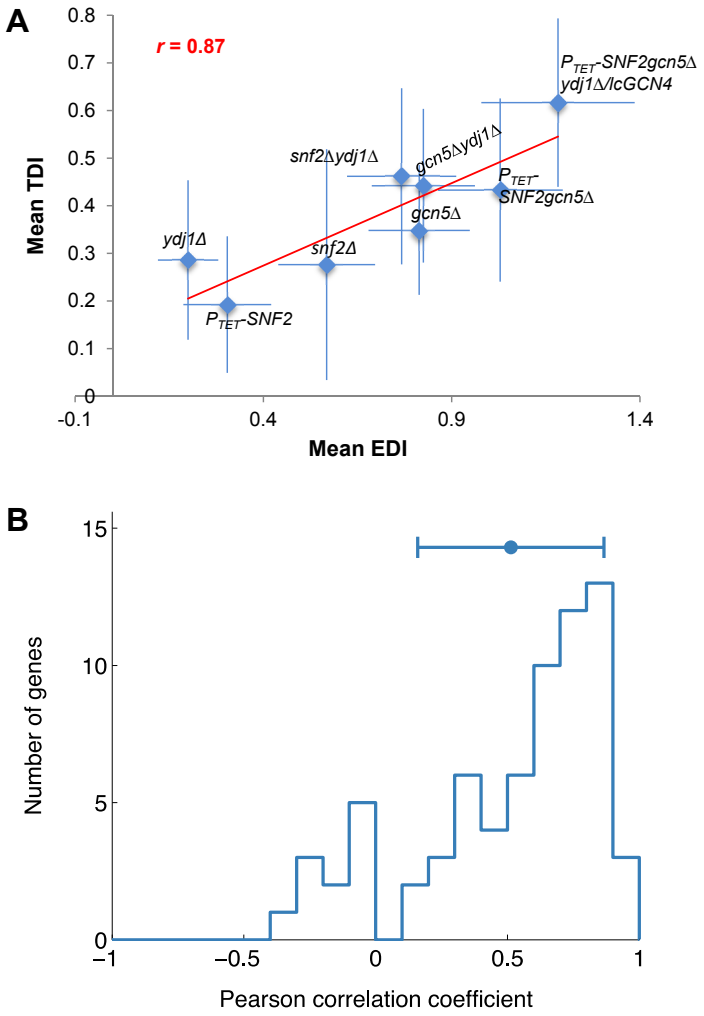

Supplemental Figure S20. Mean defects in promoter H3 eviction are associated with mean defects in Pol II induction for the group of 70 induced exemplar genes. (A) EDI/TDI values for each gene/mutant combination were calculated as in Fig. 6A-B, and the mean EDI and TDI values were calculated for the group of 70 genes and plotted (± 95% CI) for each strain, yielding the indicated Pearson's coefficient. (B) EDI and TDI values were calculated for each gene/mutant combination as in Figs. 6A-B and seventy correlation analyses were conducted for each of the 70 exemplar genes between the EDI and TDI values determined for the 8 different mutants analyzed in (A), and the Pearson's coefficient (r) was tabulated for all 70 genes. The average r value for the 70 genes is 0.51, with a standard deviation of 0.35.

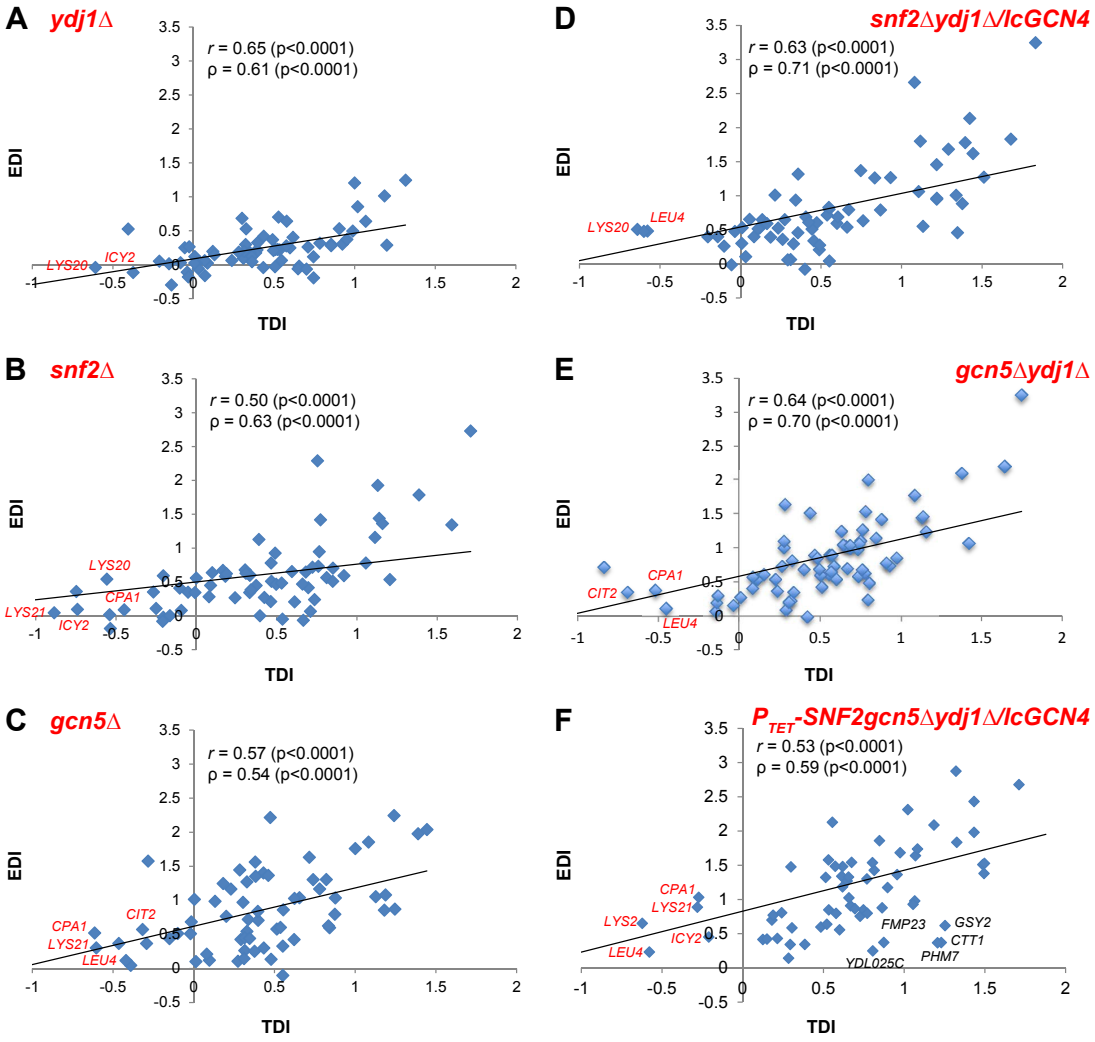

Supplemental Figure S21. Defects in promoter H3 eviction are associated with defects in Pol II induction for SM-induced exemplar genes in mutants with single, double or triple mutations eliminating or depleting Snf2, Ydj1, and Gcn5. (A-F) Scatterplots of EDIs versus TDIs calculated for all 70 exemplar SM-induced genes as in Fig. 6C, for the indicated mutants. In one or more plots, data for *RTS1*, *CIT2*, *YPS1*, *LYS20*, *LYS21*, *NRG1*, or *STE2* were omitted (but included in calculations of Pearson's (r) and Spearman's (ρ) correlation coefficients) because their large negative TDI values would confine the majority of data points to a small portion of the x-axis, as follows. (A) *ydj1*Δ: *CIT2, RTS3, YPS1*; (B) *snf2*Δ: *RTS3*; (C) *gcn5*Δ: *LYS20, RTS3*; (D) *snf2*Δ*ydj1*Δ*/lcGCN4*: *RTS3, LYS21*; (E) *gcn5*Δ *ydj1*Δ: *RTS3, LYS20*; (F) P_{TET}-*SNF2gcn5*Δ *ydj1*Δ*/lcGCN4*: *CIT2, TRS3*. In (F), *NRG1* and *STE2* were also omitted owing to their large EDI values.

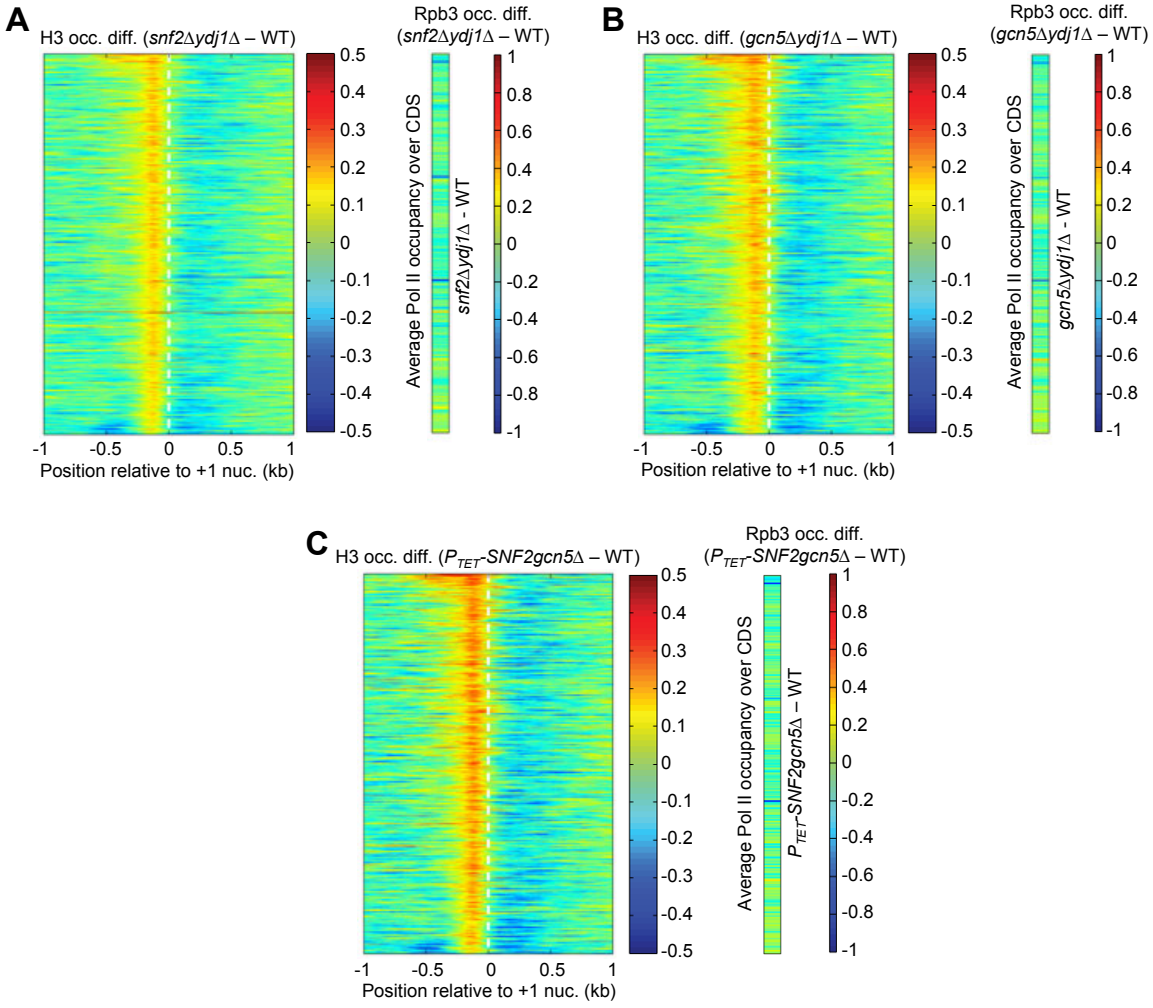

Supplemental Figure S22. Elimination of Ydj1, Snf2, Gcn5 increases H3 occupancies in the NDRs of most genes without substantially altering Pol II occupancies. (A-C) Heat maps for the identically-ordered 4744 genes shown in Fig. 7A, constructed as described in Fig. 5 for the indicated mutants.

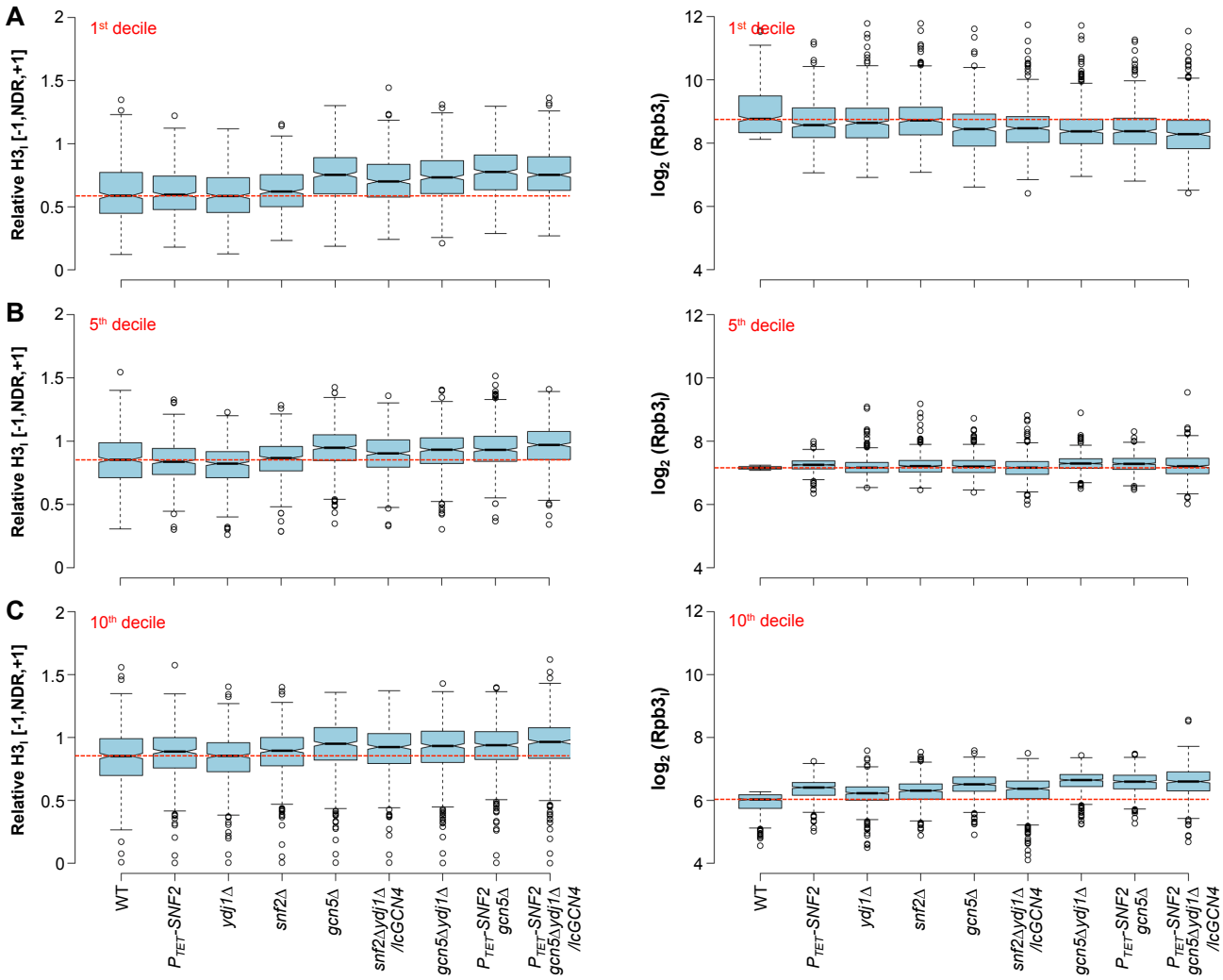

Supplemental Figure S23. Elimination of Snf2, Ydj1, or Gcn5 elevates promoter H3 occupancies genome-wide but reduces Pol II occupancies only at highly expressed genes. (A) Notched box-plots of relative H3 occupancies per bp in the [-1,NDR,+1] window (*left*) and $\log_2$ values of $Rpb3_I$ occupancies per bp in CDS (*right*) under inducing conditions for the first decile (with highest Rpb3 occupancies) of the group of 4744 weakly or non-induced genes. (B) Same as (A) except for the 5^{th} decile of Rpb3 occupancy in WT cells. (C) Same as (A) except for the tenth decile of the group of 4744 genes (with lowest Rpb3 occupancies). Averaged H3 and Rpb3 ChIP-seq data from 3 biological replicates was employed.

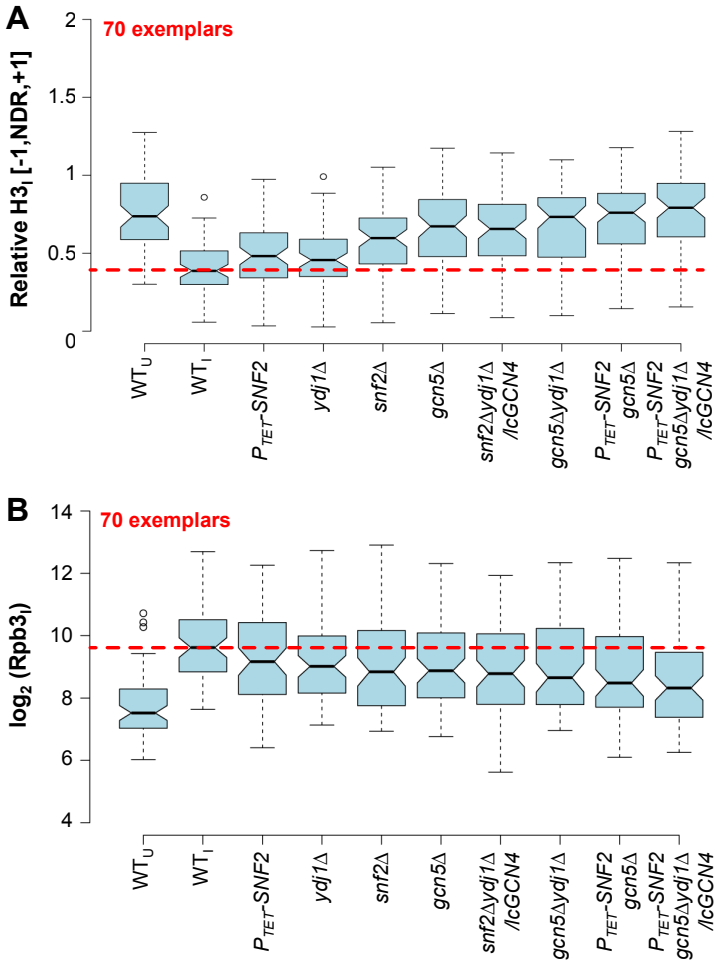

Supplemental Figure S24. Elimination of Snf2, Ydj1, or Gcn5 elevates H3 occupancies and reduces Pol II occupancies at the 70 exemplar induced genes. Notched box-plots of H3 occupancies in the [-1,NDR,+1] window (A) and $\log_2(\text{Rpb3}_\text{I})$ occupancies (B) under inducing conditions for the 70 exemplar induced genes. Data in (A) was presented in Fig. 3D and is reproduced here for comparison to (B).

Supplemental Tables

Supplemental Table S1. Yeast strains used in this study

Name	Parent	Relevant genotype[1]	Reference
BY4741[2]		*MATa his3Δ1 leu2Δ met15Δ ura3Δ*	Research Genetics
249[2]	BY4741[2]	*gcn4Δ::kanMX4*	Research Genetics
1586[2]	BY4741[2]	*snf2Δ::kanMX4*	Research Genetics
3012[2]	BY4741[2]	*ydj1Δ::kanMX4*	Research Genetics
1742[2]	BY4741[2]	*gal11Δ::kanMX4*	Research Genetics
1038[2]	BY4741[2]	*ada1Δ::kanMX4*	Research Genetics
7285[2]	BY4741[2]	*gcn5Δ::kanMX4*	Research Genetics
1310[2]	BY4741[2]	*asf1Δ::kanMX4*	Research Genetics
1490[2]	BY4741[2]	*rtt109Δ::kanMX4*	Research Genetics
5119[2]	BY4741[2]	*nap1Δ::kanMX4*	Research Genetics
5922[2]	BY4741[2]	*yta7Δ::kanMX4*	Research Genetics
771[2]	BY4741[2]	*hsc82Δ::kanMX4*	Research Genetics
1512[2]	BY4741[2]	*ssa2Δ::kanMX4*	Research Genetics
1703[2]	BY4741[2]	*htz1Δ::kanMX4*	Research Genetics
HQY1595	7285	*gcn5Δ::kanMX4 ydj1Δ::hphMX4*	This work
HQY1598	1586[2]	*snf2Δ::kanMX4 ydj1Δ::hphMX4*	This work
HQY1602	771	*hsc82Δ::kanMX4 hsp82Δ::hphMX4* pHQ2066*[LEU2 hsp82-T101I]*	This work
HQY1603	771	*hsc82Δ::kanMX4 hsp82Δ::hphMX4* pHQ2067*[LEU2 hsp82-G170D]*	This work
HQY1607	1512	*ssa1Δ::hphMX4 ssa2Δ::kanMX4*	This work
HQY1610	1586	*snf2Δ::kanMX4 yta7Δ::hphMX4*	This work
HQY1611	7285	*gcn5Δ::kanMX4 yta7Δ::hphMX4*	This work
HQY1612	1586	*snf2Δ::kanMX4 asf1Δ::hphMX4*	This work
HQY1623	7285	*HIS3*::P_{TET}-SNF2 gcn5Δ::kanMX4*	This work
HQY1625	249[2]	*HIS3*::P_{TET}-SNF2 gcn4Δ::kanMX4*	This work
HQY1627	BY4741[2]	*HIS3*::P_{TET}-SNF2*	This work
HQY1657	HQY1595	*HIS3*::P_{TET}-SNF2 gcn5Δ::kanMX4 ydj1Δ::hphMX4*	This work
BLY49	MATa	*sth1-3ts his3-Δ200 ura3-52 lys2-801 ade2-101*	Chai et al. (2005)
L577	MATα	*spt16-197 his4Δ912 lys2Δ128 ura3-52*	Malone et al. (1991)

[1] *HIS3** designates the *HIS3* allele from S. kluyveri.
[2] Strains are purchased from Research Genetics.

Supplemental Table S2. H3-PESCI studies

Yeast strain (genotype)	Sample ID	No. of aligned paired reads[1]	Pearson correlation[2] r	
			Exp. 1	Exp. 2
BY4741 (WT, uninduced)	AGH0220-1 (Exp. 1)	22,933,214		
	AGH0220-2 (Exp. 2)	20,223,628	0.958	
	AGH0220-3 (Exp. 3)	21,078,138	0.958	0.955
BY4741 (WT, induced)	AGH0220-4 (Exp. 1)	27,288,850		
	AGH0220-5 (Exp. 2)	22,101,846	0.929	
	AGH0220-6 (Exp. 3)	22,386,501	0.922	0.956
1586 (*snf2*Δ)	AGH0406-10-1 (Exp. 1)	23,691,663		
	AGH0406-10-2 (Exp. 2)	30,728,286	0.912	
	AGH25-1 (Exp. 3)	27,312,607	0.806	0.791
3012 (*ydj1*Δ)	AGH0406-11-1 (Exp. 1)	22,351,818		
	AGH0406-11-2 (Exp. 2)	23,409,609	0.928	
	AGH25-2 (Exp. 3)	26,326,214	0.858	0.864
7285 (*gcn5*Δ)	AGH08-5 (Exp. 1)	13,992,780		
	AGH09-5 (Exp. 2)	10,618,715	0.817	
	AGH25-3 (Exp. 3)	26,846,307	0.791	0.763
HQY1598 (*snf2*Δ*ydj1*Δ/*lcGCN4*)	AGH13-1 (Exp. 1)	30,295,240		
	AGH13-2 (Exp. 2)	26,707,317	0.921	
	AGH13-3 (Exp. 3)	23,557,188	0.878	0.854
HQY1595 (*gcn5*Δ*ydj1*Δ)	AGH08-6 (Exp. 1)	14,521,858		
	AGH09-6 (Exp. 2)	12,233,963	0.864	
	AGH25-4 (Exp. 3)	25,370,469	0.835	0.821
HQY1627 (P_{TET}-*SNF2*)	AGH08-4 (Exp. 1)	14,492,452		
	AGH09-4 (Exp. 2)	12,155,964	0.840	
	AGH25-8 (Exp. 3)	24,176,184	0.822	0.859
HQY1623 (P_{TET}-*SNF2gcn5*Δ)	AGH08-8 (Exp. 1)	14,462,524		
	AGH09-8 (Exp. 2)	9,372,348	0.812	
	AGH25-10 (Exp. 3)	22,921,217	0.719	0.689
HQY1657 (P_{TET}-*SNF2gcn5*Δ*ydj1*Δ/*lcGCN4*)	AGH08-12 (Exp. 1)	12,230,198		
	AGH09-12 (Exp. 2)	11,667,423	0.746	
	AGH27-5 (Exp. 3)	25,380,703	0.491	0.505

[1] Using Bowtie 2 to align reads to the SacCer2 version of the genome sequence.

[2] Pearson correlations between experiments for the H3 average occupancy in the combined [-1,NDR,+1] regions of 5403 annotated genes.

Supplemental Table S3. Rpb3-PESCI studies

Yeast strain (genotype)	Sample ID	No. of aligned paired reads[1]	Pearson correlation[2] r	
			Exp. 1	Exp. 2
BY4741 (WT, uninduced)	AGH03-1 (Exp. 1)	27,714,859		
	AGH03-2 (Exp. 2)	31,174,598	0.997	
	AGH03-3 (Exp. 3)	32,460,758	0.995	0.992
BY4741 (WT, induced)	AGH03-4 (Exp. 1)	23,003,834		
	AGH03-5 (Exp. 2)	29,921,812	0.995	
	AGH03-6 (Exp. 3)	26,823,064	0.995	0.994
249 (*gcn4*Δ)	AGH12-1 (Exp. 1)	16,573,573		
	AGH12-2 (Exp. 2)	15,234,053	0.998	
	AGH23-11 (Exp. 3)	12,149,580	0.950	0.952
1586 (*snf2*Δ)	AGH12-7 (Exp. 1)	18,787,456		
	AGH12-8 (Exp. 2)	17,401,885	0.997	
	AGH28-1 (Exp. 3)	23,806,884	0.952	0.957
3012 (*ydj1*Δ)	AGH12-9 (Exp. 1)	20,262,851		
	AGH12-10 (Exp. 2)	20,954,044	0.997	
	AGH28-2 (Exp. 3)	25,344,969	0.936	0.931
7285 (*gcn5*Δ)	AGH1018-5 (Exp. 1)	23,998,691		
	AGH1119-5 (Exp. 2)	23,412,718	0.991	
	AGH28-3 (Exp. 3)	22,255,960	0.864	0.866
HQY1598 (*snf2*Δ*ydj1*Δ/*lcGCN4*)	AGH13-4 (Exp. 1)	23,925,582		
	AGH13-5 (Exp. 2)	26,980,682	0.975	
	AGH13-6 (Exp. 3)	24,924,859	0.970	0.975
HQY1595 (*gcn5*Δ*ydj1*Δ)	AGH1018-6 (Exp. 1)	20,744,649		
	AGH1119-6 (Exp. 2)	24,995,164	0.977	
	AGH28-4 (Exp. 3)	20,314,069	0.926	0.927
HQY1627 (P_{TET}-*SNF2*)	AGH1018-4 (Exp. 1)	18,963,524		
	AGH1119-4 (Exp. 2)	25,390,805	0.980	
	AGH28-8 (Exp. 3)	23,667,405	0.950	0.959
HQY1623 (P_{TET}-*SNF2gcn5*Δ)	AGH1018-8 (Exp. 1)	20,681,102		
	AGH1119-8 (Exp. 2)	25,091,761	0.978	
	AGH28-10 (Exp. 3)	21,059,642	0.926	0.943
HQY1657 (P_{TET}-*SNF2gcn5*Δ*ydj1*Δ/*lcGCN4*)	AGH1018-12 (Exp. 1)	24,057,383		
	AGH1119-12 (Exp. 2)	20,092,762	0.970	
	AGH27-10 (Exp. 3)	28,621,240	0.840	0.855

[1] Using Bowtie 2 to align reads to the SacCer2 version of the genome sequence.

[2] Pearson correlations between experiments for the Rpb3 occupancies averaged over the CDS for all 5783 genes with the CDS longer than 170 bp.

Supplemental Table S4. Nuc-seq studies

Yeast strain (genotype)	Sample ID	No. of aligned paired reads[1]	Pearson correlation[2] r
BY4741 (WT, uninduced)	AGH01-1 (Exp. 1)	8,699,065	0.983
	AGH01-2 (Exp. 2)	8,060,225	
BY4741 (WT, induced)	AGH01-3 (Exp. 1)	7,068,815	0.987
	AGH01-4 (Exp. 2)	10,220,772	

[1] Using Bowtie 2 to align reads to the SacCer2 version of the genome sequence.

[2] Pearson correlations between experiments for the nucleosome occupancies in the 450 bp spanning nucleotides -389 to +61 (relative to the ATG codon) of each gene for all 5783 genes with the CDS longer than 170 bp.

Additional Supplemental Files

Supplemental File S1

ChIP-seq analysis of H3 and Rpb3 occupancies in uninduced and SM-induced WT cells. Sequence reads from three biological replicates were combined and H3 occupancies at each bp were normalized to the average occupancy per bp on the respective chromosome, to yield relative H3 occupancies. Rpb3 occupancies were normalized to correct for differences in total read depth in different experiments. The relative H3 occupancies per bp in the [-1,NDR,+1] intervals for each gene, identified as in Fig. S10B, are listed for all 5332 genes for which the [-1,NDR,+1] region could be defined (sheet 4), 4744 genes exhibiting $<$1.5-fold induction of Rpb3 on SM induction (sheet 3), 211 genes selected from a group of 223 exhibiting SM-induction of Rpb3 by $\geq$2-fold (sheet 2), and 70 exemplar genes from the group of 211 genes displaying an $H3_U/H3_I$ ratio of $\geq$1.415 (sheet 1). The group of 223 SM-induced genes does not include all genes exhibiting $Rpb3_I/Rpb3_U$ $\geq$2-fold as it excludes certain genes that appear to exhibit read-through transcription from adjacent, highly induced genes that does not extend across the entire CDS, or that have unusually low reads under one or both conditions. Of the 223 genes that satisfy these criteria, the [-1,NDR,+1] region could not be defined for 12 genes, yielding the group of 211 genes listed in sheet 2. Note that 14 genes in the group of 211 belong to pairs of divergently oriented genes that share a common NDR, and that one of the two genes in the pair (highlighted in yellow) was excluded in certain analyses of 204 SM-induced genes described in RESULTS. In addition, of the 73 genes from the group of 211 genes that display an $H3_U/H3_I$ ratio of $\geq$1.415 (sheet 2), 6 genes belong to pairs of divergently oriented genes that share a common NDR, such that one of the two genes in the pair (highlighted in yellow) was excluded to produce the 70 exemplar genes (sheet 1). Sheets 1-3 list the relative H3 occupancies per bp in the [-1, NDR, +1] zones under uninducing (H3-U) or inducing (H3-I) conditions, and the Rpb3 occupancies per bp averaged over the CDS under the same two conditions (Rpb3-U, Rpb3-I) for each gene. Sheet 5 summarizes results of microarray analysis of mRNA expression in WT cells treated or untreated with SM for 2h, with 1370 genes exhibiting an SM-induced increase in mRNA expression by $\geq$1.5 and 1298 genes with a similar fold reduction in expression. Four independent RNA preparations were made from untreated or SM-treated WT cells and used for 4 microarray hybridizations, including two dye swaps, to generate mean values calculated from the 4 replicate experiments (columns F and L) (Saint et al. 2014).

Supplemental File S2

Average H3 occupancies of -1, NDR, and +1 zones in WT and mutant cells. Relative H3 occupancies were calculated from the data combined from 3 biological replicates as described in File S1. Sheets 2-17: Relative H3 occupancy per bp (Avg. H3 Occ.) was calculated for each gene for the [-1,NDR,+1] combined zones (sheets *_3zones), or individual -1 nucleosome regions (sheets *_-1), NDRs (sheets *_NDR), or +1 nucleosome regions (sheets *_+1), for WT uninduced or induced cells and the indicated 8 mutants cultured under inducing conditions in the groups of 70, 204, 4744 or all (5403) genes. Sheet 1: Mean ($\pm$ 95% CI) Avg. H3 Occs. values were calculated for the indicated gene sets (70, 204, 4744 or all 5403) in the indicated strains, along with the fold-changes in mean values between mutant and induced WT cells (rel to WT-I). The mean values ($\pm$ 95% CI) calculated for the individual -1, NDR, and +1 zones for the 70 exemplar genes are plotted in Fig. 3E.

Supplemental File S3

Summary of effects of single or double mutations that eliminate Snf2, Ydj1, or Gcn5 on promoter H3 occupancies of 70 induced exemplar genes. (Sheet 1) Compilation of p-values from Student's *t*-tests conducted on results shown in Fig. S13. Asterisks and muted colors indicate gene/mutant combinations where H3 occupancies are reduced in the mutant, indicating defects in nucleosome replacement versus eviction. Dependence on Snf2 or Ydj1 for nucleosome eviction is summarized for each gene in columns 8 or 9 using the color code at the bottom signifying p-value ranges for the comparison yielding the most significant difference between strains containing or lacking *SNF2* or *YDJ1*, which are tabulated in the preceding 5 columns. Totals for each column are listed at the bottom. (Sheet 2) Same as sheet 1 but for mutants lacking *GCN5* and *YDJ1* and compiled from *t*-tests conducted on results shown in Fig. S14.

Supplemental File S4

ChIP-seq analysis of Rpb3 occupancies averaged over the CDS in SM-induced WT and mutant cells. Rpb3 occupancy data from 3 biological replicates, from reads of 50-300 bp sequenced fragments, were normalized for differences in total read number, averaged, and normalized to CDS length, to yield the mean values listed here for all 5783 genes (sheet 4), 4744 genes exhibiting <1.5-fold induction of Rpb3 on SM induction (sheet 3), 211 genes selected from a group of 223 exhibiting SM-induction of Rpb3 by ≥2-fold (sheet 2), and 70 exemplar genes from the group of 211 genes displaying an $H3_U/H3_I$ ratio of ≥1.415 (sheet 1).

Supplemental File S5

EDI and TDI values for 70 exemplar genes. (Sheet 1) Mean (± SEM) EDI and TDI values calculated for each gene in the P_{TET}-*SNF2 gcn5*Δ double mutant by averaging EDI and TDI values calculated from three biological replicates, for the analysis in Fig. 6C. (Sheet 2) EDI and TDI values were calculated for each gene/mutant combination using the average of H3 or Rpb3 ChIP-seq data from three biological replicates for the analyses in Figs. 6A-B, S17, S20A-B, and S21A-F.

Supplemental File S6

Perl and MATLAB scripts used in this study. Archive `File S6.zip` contains two folders, `Perl_scripts` and `MATLAB_scripts`, with the Perl and MATLAB scripts used in this study. `Perl_scripts` folder contains the scripts necessary to size-select the raw paired-end reads according to the insert sizes, and to compute the number of mapped reads over promoters, coding regions, and downstream regions (see `demo.docx` for a short tutorial with the necessary steps to process the `*.sam` files containing the aligned paired-end reads that were generated with Bowtie 2). `MATLAB_scripts` folder contains the following scripts: `Detect_NDRs_and_flanking_nucleosomes` detects the locations of the nucleosome depleted regions and the flanking nucleosomes (+1/-1) corresponding to each gene promoter; `Compute_H3_averages_TSS` generates Excel tables with the genome-wide average H3 occupancy in the window [TSS-1000, TSS+1000]; `Compute_H3_averages_3_zones` generates Excel tables with the average H3 occupancy in the three zones (-1 nucleosome, NDR, +1 nucleosome) for every gene.

Supplemental References

Bellí G, Garí E, Aldea M, and Herrero E. 1998. Functional analysis of yeast essential genes using a promoter-substitution cassette and the tetracycline-regulatable dual expression system. *Yeast* **14**: 1127–1138.

Chai B, Huang J, Cairns BR, and Laurent BC. 2005. Distinct roles for the RSC and Swi/Snf ATP-dependent chromatin remodelers in DNA double-strand break repair. *Genes Dev.* **19**: 1656–1661.

Cole HA, Howard BH, and Clark DJ. 2012. Genome-wide mapping of nucleosomes in yeast using paired-end sequencing. *Methods Enzymol.* **513**: 145–168.

Cole HA, Ocampo J, Iben JR, Chereji RV, and Clark DJ. 2014. Heavy transcription of yeast genes correlates with differential loss of histone H2B relative to H4 and queued RNA polymerases. *Nucleic Acids Res.* **42**: 12512–12522.

Goldstein AL and McCusker JH. 1999. Three new dominant drug resistance cassettes for gene disruption in Saccharomyces cerevisiae. *Yeast* **15**: 1541–1553.

Longtine MS, McKenzie III A, Demarini DJ, Shah NG, Wach A, Brachat A, Philippsen P, and Pringle JR. 1998. Additional modules for versatile and economical PCR-based gene deletion and modification in Saccharomyces cerevisiae. *Yeast* **14**: 953–961.

Malone EA, Clark C, Chiang A, and Winston F. 1991. Mutations in SPT16/CDC68 suppress cis- and trans-acting mutations that affect promoter function in Saccharomyces cerevisiae. *Mol. Cell. Biol.* **11**: 5710–5717.

Saint M, Sawhney S, Sinha I, Singh RP, Dahiya R, Thakur A, Siddharthan R, and Natarajan K. 2014. The TAF9 C-terminal conserved region domain is required for SAGA and TFIID promoter occupancy to promote transcriptional activation. *Mol. Cell. Biol.* **34**: 1547–1563.

Swanson MJ, Qiu H, Sumibcay L, Krueger A, Kim Sj, Natarajan K, Yoon S, and Hinnebusch AG. 2003. A multiplicity of coactivators is required by Gcn4p at individual promoters in vivo. *Mol. Cell. Biol.* **23**: 2800–2820.

Winzeler EA, Shoemaker DD, Astromoff A, Liang H, Anderson K, Andre B, Bangham R, Benito R, Boeke JD, Bussey H, et al.. 1999. Functional characterization of the S. cerevisiae genome by gene deletion and parallel analysis. *Science* **285**: 901–906.

Xu Z, Wei W, Gagneur J, Perocchi F, Clauder-Münster S, Camblong J, Guffanti E, Stutz F, Huber W, and Steinmetz LM. 2009. Bidirectional promoters generate pervasive transcription in yeast. *Nature* **457**: 1033–1037.